Wide-Ranging Effects of the Yeast Ptc1 Protein Phosphatase Acting Through the MAPK Kinase Mkk1

Laura Tatjer,* Almudena Sacristán-Reviriego,†,1 Carlos Casado,*,2 Asier González,*,3 Boris Rodríguez-Porrata,* Lorena Palacios,† David Canadell,* Albert Serra-Cardona,* Humberto Martín,† María Molina,†,4 and Joaquín Ariño*,4

*Institut de Biotecnologia i Biomedicina and Departament de Bioquímica i Biologia Molecular, Universitat Autònoma de Barcelona, Bellaterra 08193, Barcelona, Spain, and †Departamento de Microbiología II, Facultad de Farmacia, Universidad Complutense and Instituto Ramón y Cajal de Investigaciones Sanitarias (IRYCIS), 28040 Madrid, Spain

ORCID IDs: 0000-0003-0074-3309 (M.M.); 0000-0002-6774-2987 (J.A.)

ABSTRACT The *Saccharomyces cerevisiae* type 2C protein phosphatase Ptc1 is required for a wide variety of cellular functions, although only a few cellular targets have been identified. A genetic screen in search of mutations in protein kinase–encoding genes able to suppress multiple phenotypic traits caused by the *ptc1* deletion yielded a single gene, *MKK1*, coding for a MAPK kinase (MAPKK) known to activate the cell-wall integrity (CWI) Slt2 MAPK. In contrast, mutation of the *MKK1* paralog, *MKK2*, had a less significant effect. Deletion of *MKK1* abolished the increased phosphorylation of Slt2 induced by the absence of Ptc1 both under basal and CWI pathway stimulatory conditions. We demonstrate that Ptc1 acts at the level of the MAPKKs of the CWI pathway, but only the Mkk1 kinase activity is essential for *ptc1* mutants to display high Slt2 activation. We also show that Ptc1 is able to dephosphorylate Mkk1 *in vitro*. Our results reveal the preeminent role of Mkk1 in signaling through the CWI pathway and strongly suggest that hyperactivation of Slt2 caused by upregulation of Mkk1 is at the basis of most of the phenotypic defects associated with lack of Ptc1 function.

KEYWORDS synthetic genetic interactions; cell-wall integrity pathway; protein dephosphorylation; *Saccharomyces cerevisiae*

PROTEIN kinases play an essential role in nearly every aspect of cell physiology, and the activity of these key players is frequently modulated by phosphorylation. Therefore, protein phosphatases (PPases) are important regulators of protein kinases and cellular homeostasis. Among them, type 2C Ser/Thr PPases constitute an evolutionarily conserved group that, in contrast to other PPase families, are monomeric enzymes apparently lacking regulatory subunits. In the yeast *Saccharomyces cerevisiae*, seven members (Ptc1–Ptc7) have been identified and at least partially characterized [see Arino *et al.* (2011) for a review].

Ptc1 is the closest homolog of human Wip1, a phosphatase involved in the regulation of stress-induced and DNA damage–induced networks in diverse physiologic and pathologic conditions (Le Guezennec and Bulavin 2010; Zhu and Bulavin 2012) and by far the most widely studied yeast isoform. Both the large number of characteristic phenotypes and the specific changes in the transcriptomic profile (Gonzalez *et al.* 2006) derived from deletion of the gene suggest that this phosphatase is involved in a large variety of cellular processes not shared by other Ptc family members. Early evidence indicated that Ptc1 was involved in the negative regulation of the high-osmolarity glycerol (HOG) pathway (Maeda *et al.* 1993; Maeda *et al.* 1994), and subsequent work demonstrated that Ptc1 could dephosphorylate the Hog1 MAPK *in vitro* and *in vivo* (Warmka *et al.* 2001). Ptc1 physically

doi: 10.1534/genetics.115.183202
Manuscript received September 29, 2015; accepted for publication November 2, 2015; published Early Online November 5, 2015.
Supporting information is available online at www.genetics.org/lookup/suppl/doi:10.1534/genetics.115.183202/-/DC1
[1]Present address: Institute of Ophthalmology, University College London, United Kingdom WC1E 6BT.
[2]Present address: Evolva Biotech A/S, 2200 Copenhagen, Denmark.
[3]Present address: Biozentrum, University of Basel, 4056 Basel, Switzerland.
[4]Corresponding authors: Institut de Biotecnologia i Biomedicina, UAB, Cerdanyola del Vallès, Barcelona 08193, Spain. E-mail: Joaquin.Arino@uab.es; and Departamento de Microbiología II, Facultad de Farmacia, Universidad Complutense, Plaza de Ramón y Cajal s/n 28040 Madrid, Spain. E-mail: molmifa@ucm.es

interacts with the N-terminal domain of Nbp2, an SH3 domain–containing protein that serves as an adaptor for the recruitment of Ptc1 to the Pbs2-Hog1 complex, and this interaction is necessary for Ptc1 to participate in the regulation of HOG-mediated signaling (Uetz *et al.* 2000; Ito *et al.* 2001; Mapes and Ota 2004).

Cells lacking Ptc1 display many phenotypes that cannot be explained by a Hog1-dependent role of this phosphatase. For instance, these cells are sensitive to diverse cations, including calcium (likely by hyperactivation of calcineurin phosphatase), zinc, and cesium (Gonzalez *et al.* 2006), as well as to alkaline pH (Serrano *et al.* 2004). These are traits commonly found in mutants with impaired vacuolar function, and indeed, the *ptc1* mutant displays fragmented vacuoles, mimicking those of class B *vps* (vacuolar protein–sorting) mutants (Bonangelino *et al.* 2002; Seeley *et al.* 2002; Sambade *et al.* 2005; Gonzalez *et al.* 2006). Deletion of *PTC1* confers a lithium (but not sodium)–sensitive phenotype. This can be attributed, at least in part, to a less effective cation extrusion, likely due to a Hog1-independent decrease in the expression of the Na^+-ATPase *ENA1* gene (Ruiz *et al.* 2006).

Ptc1 is required for the correct inheritance of organelles such as vacuoles, mitochondria, cortical endoplasmic reticulum (ER), peroxisomes, and secretory vesicles. These effects are independent of Hog1 dephosphorylation (Roeder *et al.* 1998; Du *et al.* 2006; Jin *et al.* 2009). Moreover, lack of Ptc1 results in additional phenotypic traits, such as defects in transfer RNA (tRNA) splicing and growth in nonfermentable media (Robinson *et al.* 1994) and, in haploid strains, cell separation defects and a random budding pattern at 37° (Gonzalez *et al.* 2006). A link between Ptc1 and the target-of-rapamycin (TOR) pathway was suggested by the increased sensitivity of *ptc1* cells to rapamycin, an inhibitor of the TORC1 complex (Parsons *et al.* 2004; Xie *et al.* 2005). Subsequent work demonstrated that Ptc1 is required for normal TOR signaling by regulating, in a HOG-independent manner, a step upstream of the Sit4 phosphatase (Gonzalez *et al.* 2009). Recently, Ptc1 has been shown to dephosphorylate the Snf1 protein kinase at Thr 210 *in vivo* (Ruiz *et al.* 2013).

Early work showed that mutations in *PTC1* could suppress phenotypes derived from hypoactive *pkc1* alleles (Huang and Symington 1995), thus pointing to a link between Ptc1 and the cell-wall integrity (CWI) pathway. This pathway is composed of several membrane sensors that signal through the small GTPase Rho1 to the Pkc1 kinase. Pkc1 is the upstream element of a MAPK cascade composed by the MAPK kinase kinase (MAPKKK) Bck1 that phosphorylates two similar MAPKKs (Mkk1 and Mkk2), which, in turn, phosphorylate and activate the MAPK Slt2. Phosphorylation of Slt2 occurs at Tyr and Thr residues in a T-X-Y motif within the activation loop common to MAPKs [see Levin (2011) for a review]. In keeping with the involvement of Ptc1 in the CWI pathway, *ptc1* mutants are sensitive to diverse cell-wall antagonists such as calcofluor white (CFW), Congo red, caffeine, and caspofungin (Ram *et al.* 1994; Markovich *et al.* 2004; Sharmin *et al.* 2014) or to other conditions that activate the CWI pathway, such as alkaline pH (Serrano *et al.* 2004, 2006). In addition, the *ptc1* mutation is synthetically lethal with mutations in genes that are important for cell-wall construction, such as *FKS1*, *GAS1*, and *SMI1* (Lesage *et al.* 2004). Despite the known crosstalk between the Slt2 and HOG pathways (Hahn and Thiele 2002; Bermejo *et al.* 2008), the hypersensitivity of the *ptc1* strain to cell-wall-damaging agents does not involve hyperactivation of Hog1 (Gonzalez *et al.* 2006). Cells lacking Ptc1 display higher than normal amounts of active Slt2 (Du *et al.* 2006; Gonzalez *et al.* 2006) and show increased expression of diverse genes (*MLP1*, *CRH1*, and *SED1*) regulated by the Slt2 MAPK module (Gonzalez *et al.* 2006). More recently, Nbp2 has been described to mediate the interaction between Ptc1 and different kinases, including Bck1 (Hruby *et al.* 2011; Stanger *et al.* 2012). In agreement, elimination of Nbp2 results in increased sensitivity to cell-wall stressors. All this evidence suggests that Ptc1 could dephosphorylate members of the Slt2 pathway through this adaptor, contributing to the downregulation of the cascade, although the precise target(s) are yet unknown.

Based on the concept that the phenotypes observed in *ptc1* mutants could be derived from the hyperphosphorylation of specific direct or indirect Ptc1 targets, we subjected a collection of mutants combining the absence of Ptc1 with that of nonessential genes encoding protein kinase catalytic or regulatory subunits to an array of phenotypic tests in search of genetic interactions, particularly those resulting in the rescue of a wide variety of *ptc1* defects. Interestingly, only the mutation of one protein kinase gene, *MKK1*, contributed to the normalization of all *ptc1* phenotypes tested. In this paper, we provide biochemical and genetic evidence showing that Mkk1 transmits most of the signaling through the CWI pathway and that Ptc1 directly downregulates the CWI pathway at the level of the MAPKKs. We propose that abnormal activation of the Slt2 kinase caused by deregulation of Mkk1 would be responsible for most phenotypic traits displayed by *ptc1* mutant cells.

Materials and Methods

Media and growth conditions

Yeast cells were grown at 28° in YPD medium (10 g/l yeast extract, 20 g/l peptone, and 20 g/l dextrose) or, when carrying plasmids, in synthetic complete medium (Adams *et al.* 1997) containing 2% glucose and lacking the appropriate selection requirements. *Escherichia coli* DH5α cells were used as the plasmid DNA host and were grown at 37° in LB broth supplemented with 50 μg/ml of ampicillin, when required.

Strains and gene disruptions

Strains used to generate double mutants for screen purposes derive from wild-type strains BY4741 and BY4742, MAR143 (BY4741 *ptc1*::*nat1*), or MAR216 (BY4742 *ptc1*::*nat1*), generated by transformation of BY4742 wild-type cells with the *ptc1*::*nat1* disruption cassette (Ruiz *et al.* 2006). Single

BY4741 *KanMX4* kinase deletion mutants correspond to the Saccharomyces Genome Deletion Collection (Winzeler *et al.* 1999) from EUROSCARF. A subset of double mutants (59 strains) was obtained by crossing the kinase mutants with strain MAR216. Homozygous double mutants were recovered by random spore or tetrad analysis. Thirty-four double mutants were generated by transformation with the *ptc1*::*nat1* disruption cassette and selection with 100 μg/ml of nourseothricin (Werner BioAgents). Finally, 22 double mutants were generated by amplifying the kinase disruption cassettes from the single *kanMX4* mutants and introducing them into strain MAR143. Positive clones were selected in the presence of 200 μg/ml of G418 (Calbiochem). Strains YPL14 and YPL15, carrying the disruption of *PTC1* in the single *mkk1* and *mkk2* mutant strains, respectively (BY4741 background), were obtained by replacement of the wild-type *PTC1* gene by the *Sna*BI/*Sph*I *ptc1*::*HIS3* fragment from the pGEMT-*ptc1*::*HIS3* plasmid (see later) selected in the absence of histidine and checked by PCR with oligonucleotides FPTC1 and RPTC1. Strains AGS33 and AGS34 were prepared by transformation of the *cch1*::*KanMX4* and *mid1*::*KanMX4* deletion mutants, respectively, with the *ptc1*::*nat1* disruption cassette described earlier. These specific strains are listed in Table 1. All other yeast strains are listed in Supporting Information, Table S1. Oligonucleotides used in this study are listed in Table S2.

Plasmids

Overexpression of GST-Slt2 was carried out from plasmid pEGH-GST-SLT2 (Zhu *et al.* 2000). Expression of $PKC1^{AAA}$ and *BCK1-20* was achieved using YEplac112-$PKC1^{A398A405A406}$ and pRS316-*BCK1-20* (Martin *et al.* 2000). Plasmids pRS416-*MKK1*myc, pRS416-*MKK2*myc, pRS416-$MKK1^{K250R}$myc, pRS416-$MKK2^{K243R}$myc (Jimenez-Sanchez *et al.*, 2007), and pYES3-$BCK1^{CT}$ (Sacristan-Reviriego *et al.* 2015) have been described previously. To overexpress GST-Ptc1 and GST-Nbp2, the *PTC1* and *NBP2* ORFs were, respectively, PCR amplified using genomic DNA as a template with primers FPTC1 and RPTC1 or FNBP2 and RNBP2. Then the *Bam*HI-digested fragments were subcloned into pEG(KG) (Mitchell *et al.* 1993), generating plasmids pEG(KG)-*PTC1* and pEG(KG)-*NBP2*. To overexpress Ptc1 fused to GFP in N- and C-terminal positions, the pYES3-*GFP-PTC1* and YCplG-*PTC1-GFP* plasmids were constructed by subcloning the *Bam*HI-digested *PTC1* ORF into pYES3-GFP (Andrés-Pons *et al.* 2007) and YCplG-GFP (Rodriguez-Escudero *et al.* 2006), respectively. The pGEMT-*ptc1*::*HIS3* plasmid was obtained by subcloning the *Sma*I-digested *HIS3* ORF from plasmid p34H-*HIS3* into the *Stu*I site of plasmid pGEMT-*PTC1*, which was made using the same *PTC1* PCR product described earlier. To construct plasmid pEG(KG)-$MKK1^{S386P}$, the $MKK1^{S386P}$ ORF was amplified by PCR using the plasmid pNV7W-$MKK1^{P386}$ (Watanabe *et al.* 1995) as template and employing primers FMKK1 and RMKK1. The *Sal*I-digested fragment was cloned into pEG(KG).

Plasmid pGEX-6P1-PTC1 was used to generate recombinant Ptc1 enzyme as a GST fusion. This plasmid was constructed by amplification of the *PTC1* ORF with oligonucleotides PTC1_pGEX-Fw and PTC1_pGEX_Rv, digestion of the amplification fragment with *Sal*I and *Bam*HI, and cloning into the same sites of plasmid pGEX-6P1. Bacterial expression of GST-Mkk1 was accomplished using plasmid pGEX(KG)-MKK1, as described in Jimenez-Sanchez *et al.* (2007).

Phenotypic screen of the ptc1-kinase gene double-mutant collection

The collection of double mutants was analyzed for tolerance to diverse conditions by drop tests (dilutions of OD_{660} = 0.05, 0.01, and 0.002) on YPD plates containing LiCl (50, 75, 100, 150, and 200 mM), calcofluor white (1, 2.5, 5, 10, and 15 μg/ml), caffeine (2.5, 5, 7.5, 10, and 15 mM), rapamycin (2.5, 5, 7.5, 10, and 15 ng/ml), $CaCl_2$ (50, 100, 150, 200, and 400 mM), and $ZnCl_2$ (1, 2, 4, and 6 mM) or adjusted with TAPS to pH 7.8, 7.9, 8.0, 8.1, and 8.2. Growth on ethanol as the only carbon source was tested on YP plates containing 2% ethanol. Plates were incubated for 72 hr, and growth was recorded. For evaluation of the genetic interactions, a semi-quantitative score was defined, as reported previously (Barreto *et al.* 2011) (see also *Results*).

β-Galactosidase reporter assays

Cells carrying plasmids pGAP1 and pMEP1 (Gonzalez *et al.* 2009), pKC201 (Alepuz *et al.* 1997), pMLP1-LacZ (Garcia *et al.* 2009), and pAMS366 (Stathopoulos and Cyert 1997) were grown to saturation on synthetic medium lacking uracil or, in the case of pMEP2 (Marini *et al.* 1997), lacking leucine and then inoculated into 5 ml of YPD medium up to an OD_{660} of 0.2. Growth was resumed until an OD_{660} of 0.8 was reached. Then aliquots of 1 ml were centrifuged and resuspended in the same volume of the appropriate YPD medium (noninduced cells), YPD medium containing 200 ng/ml of rapamycin (pGAP1, pMEP1, and pMEP2), 30 μg/ml of Congo red (pMLP1-LacZ), or 0.2 M LiCl (pKC201). Growth was resumed for 60 min (pGAP1 and pKC201), 90 min (pMEP1 and pMEP2), or 180 min (pMLP1-LacZ). pAMS366-based assays were as in Gonzalez *et al.* (2006). Finally, cells were collected, and β-galactosidase activity was measured (Reynolds *et al.* 1997).

Flow cytometric assays

For monitoring effects on cell cycle, 10 ml of the appropriate cultures were grown up to exponential phase (OD_{660} = 0.6) and split in two aliquots, and one aliquot was given 5 μg/ml of CFW. At given times, 1 ml of culture was taken and centrifuged (1800 × *g* for 2 min). The supernatant was removed and the cells resuspended in 1 ml of 70% ethanol and stored at 4° for further use. Then cells were recovered by centrifugation (1800 × *g* for 2 min), washed twice with 1 ml of 50 mM Tris-HCl (pH 7.8), and resuspended in 1 ml of the same solution containing 200 μg/ml of RNAse A. Samples were incubated for 2 hr at 37°, spun down, resuspended with 0.5 ml of freshly prepared pepsin solution (5 mg/ml in 50 mM HCl), and incubated at 37° for 30 min. Cells were recovered by centrifugation, washed with 1 ml of FACS buffer

(200 mM Tris-HCl, pH 7.5, 211 mM NaCl, and 78 mM $MgCl_2$), and resuspended in 0.5 ml of FACS buffer plus 55 μl of a 0.5 mg/ml propidium iodide solution. Samples then were processed for FACS analysis in a FACSCalibur apparatus (BD Biosciences). Distribution of the population along the cell cycle was determined with FlowJo software (v8.7) and the Dean-Jett-Fox algorithm.

For Mlp1-GFP expression analysis, cells transformed with pMLP1-GFP (Rodriguez-Peña *et al.* 2008) were collected, washed twice with PBS, and then analyzed by flow cytometry in a Guava easyCyte flow cytometer (Millipore) with a laser at 488-nm excitation and a 525/30 BP emission filter (BFP). The marker was yeast cells that did not express GFP.

Glutathione Sepharose protein purification and mass spectrometry (MS) analysis

Expression of GST-Slt2 from the pEGH-GST-SLT2 plasmid (*GAL1* promoter) was achieved by shifting cells from synthetic medium lacking uracil with glucose to the same medium with raffinose (OD_{660} = 0.6). Cultures were grown until OD_{660} = 1.2–1.4, and then 2% galactose was added and growth resumed for 5–6 hr. To activate the Slt2 cascade, some cultures were subjected to alkaline pH stress (pH 8.2) for 10 min. Cultures were filtered, washed with prechilled water, snap frozen, and kept at −80°. To purify the GST-Slt2 protein, the crude protein extract (Martin *et al.* 2000) was incubated with 125 μl of a slurry of Glutathione Sepharose beads (Amersham Biosciences) overnight at 4° with gentle shaking. Samples were centrifuge, and the supernatant was removed. Beads were resuspended in 200 μl of lysis buffer and transferred to MultiScreen filter plates (Millipore). Proteins retained were fractionated by SDS-PAGE, followed by Coomassie staining. Tryptic peptides from the relevant bands were analyzed by MS. Phosphopeptides were enriched with the TiO_2 Enrichment Kit (Calbiochem). The resulting peptides were analyzed by matrix-assisted laser desorption/ionization–time-of-flight (MALDI-TOF) MS, and mass spectra were recorded in the positive-ion mode on an UltrafleXtreme mass spectrometer (Bruker Daltonics) externally calibrated using a standard peptide mixture.

Immunoblotting analysis

For immunoblotting purposes, protein extracts were prepared as described previously (Martin *et al.* 2000; Serrano *et al.* 2006). Immunodetection of glucose-6-phosphate dehydrogenase (G6PDH) and Myc-tagged proteins was carried out using polyclonal anti-G6PDH (Sigma) and monoclonal 4A6 (Millipore) antibodies, respectively. Polyclonal anti-phospho-p44/p42 MAPK (Thr202/Tyr204) (Cell Signaling) and anti-GST (Santa Cruz Biotechnology) antibodies were used as described by Martin *et al.* (2000). Immunodetection of GFP and actin was performed using monoclonal anti-GFP (Clontech) and anti-actin C4 (MP Biomedicals) antibodies. Polyclonal anti-phospho-p38 (Thr180/Tyr182) (Cell Signaling) antibody also was employed. The primary antibodies were detected using a fluorescently conjugated secondary antibody with an Odyssey Infrared Imaging System (LI-COR Biosciences).

Expression of recombinant GST-Ptc1 and GST-Mkk1

In brief, expression of recombinant GST-Ptc1 and GST-Mkk1 was made as follows: *E. coli* BL21 (DL3) cells transformed with plasmids pGEX-6P1-PTC1 and pGEX(KG)-MKK1, respectively, were induced with 0.1 mM isopropyl β-D-1-thiogalactopyranoside (IPTG) and grown overnight at 20°. The collected cells were disrupted by sonication (Bioruptor) in buffer M [50 mM Tris/HCl, pH 7.5, 150 mM NaCl, 10% glycerol, 0.1% Triton X-100, 2 mM DTT, 0.5 phenylmethylsulfonyl fluoride (PMSF), and a protease inhibitor cocktail (Roche)], supplemented with 2 mM $MnCl_2$ in the case of GST-Ptc1 expression, and allowed to bind overnight at 4° to equilibrated Glutathione Sepharose 4B resin (GE Healthcare), followed by extensive washing with buffer M (without protease inhibitors).

For GST-Mkk1 preparation, the beads were washed three times with buffer K [25 mM MOPS, pH 7.5, 10 mM $MgCl_2$, 1 mM Na_3VO_4, 15 mM p-nitrophenyl phosphate (pNPP), and 50 mM β-glycerophosphate], resuspended (50% slurry) in the same buffer containing 30% glycerol, and stored at −20° until use. For Ptc1, the beads were washed extensively with buffer M (without protease inhibitors), followed by four washes with the same buffer lacking Triton X-100 and two washes with PreScission buffer (50 mM Tris-HCl, pH 7, 150 mM NaCl, 1 mM EDTA, and 1 mM DTT). The beads then were treated with PreScission Protease (50 units per milliliter of beads) overnight at 4°. The released protein was recovered with the supernatant, glycerol was added up to 10%, and samples were stored at −80° until use.

Expression and purification of recombinant Ppz1 were performed as described by Garcia-Gimeno *et al.* (2003), except that induction was carried out overnight at 21° and EGTA was omitted from the lysis buffer.

In vitro dephosphorylation of Mkk1

Yeast extracts used for *in vitro* phosphorylation of GST-Mkk1 bound to the affinity beads were prepared as follows: 50-ml cultures ($OD_{660} \approx 0.8$) of a *slt2* deletion mutant in the BY4741 background, transformed with plasmid pRS316-Bck1-20, were subjected to heat shock (39°) for 1 hr. Cells were collected and resuspended in 450 μl of buffer L [50 mM Tris-HCl, pH 7.5, 5% glycerol, 100 mM NaCl, 0.1% Nonidet P-40, 10 mM NaF, 1 mM Na_3VO_4, 15 mM $Na_4P_2O_7$, 15 mM pNPP, complete EDTA-free protease inhibitor (Roche), and 1 mM PMSF]. Then 200 μl of glass beads was added, and the cells were lysed in a FastPrep apparatus (five rounds of 20 sec at setting 5.0, storing samples for 1 min on ice between rounds). The lysate was centrifuged for 15 min at 12,000 × *g* at 4°, and the supernatant was recovered and stored in aliquots at −80°.

For *in vitro* dephosphorylation assays of Mkk1 by Ptc1, 100 μl of the GST-Mkk1 slurry (containing approximately

Table 1 Strains used in this work

Strain	Genotype	Source or Reference
CML128	*MAT***a** *leu2-3,112 ura3-52 trp1 his4 can*	de la Torre-Ruiz *et al.* (2002)
MML344	CML128 *pkc1*::*LEU2*	de la Torre-Ruiz *et al.* 2002)
YPH499	*MAT***a** *ade2-101 trp-63 leu2-1 ura3-52 his3-Δ200 lys2-801*	P. Hieter gift
YMJ1	YPH499 *mkk1*::*KanMX4*	Jimenez-Sanchez *et al.* (2007)
YMJ2	YPH499 *mkk2*::*SpHIS5*	Jimenez-Sanchez *et al.* 2007)
BY4741	*MAT***a** *his3Δ1 leu2Δ met15Δ ura3*	Brachmann *et al.* (1998)
BY4742	*MATα his3Δ1 leu2Δ0 lys2Δ0 ura3Δ0*	Brachmann *et al.* (1998)
Y03520	BY4741 *nbp2*::*KanMX4*	EUROSCARF
Y01328	BY4741 *bck1*::*KanMX4*	EUROSCARF
Y02487	BY4741 *mkk1*::*KanMX4*	EUROSCARF
Y02112	BY4741 *mkk2*::*KanMX4*	EUROSCARF
MAR143	BY4741 *ptc1*::*nat1*	Ruiz *et al.* (2006)
MAR216	BY4742 *ptc1*::*nat1*	Ruiz *et al.* (2006)
YPL14	BY4741 *mkk1*::*KanMX4 ptc1*::*HIS3*	This work
YPL15	BY4741 *mkk2*::*KanMX4 ptc1*::*HIS3*	This work
AGS33	BY4741 *cch1*::*KanMX4 ptc1*::*nat1*	This work
AGS34	BY4741 *mid1*::*KanMX4 ptc1*::*nat1*	This work

The collection of double *ptc1*-kinase mutants used for the screen is listed in Table S1.

13 μg of GST-Mkk1) or the equivalent amount of slurry carrying GST was mixed with 20 μl of a solution containing 125 mM MOPS (pH 7.5), 250 mM NaF, 250 mM β-glycerophosphate, and 25 mM sodium pyrophosphate; 10 μl of 200 mM $MgCl_2$; 20 μl of 1 mM ATP; 12 μl of [γ-^{32}P]-ATP (3000 Ci/mmol, 10 mCi/ml), and 33 μl of the cell extract described earlier (~450 μg of protein). The suspension was adjusted to 200 μl with water and incubated for 1 hr at 30°. Samples were centrifuged, the supernatant removed, and the beads washed twice with cold 25 mM MOPS (pH 7.5) and 50 mM NaF buffer; twice with 25 mM MOPS (pH 7.5), 100 mM NaCl, 5 mM EGTA, and 2 mM DTT buffer; and twice with buffer P (50 mM Tris-HCl, pH 7, 0.1 mM EGTA, 20 mM $MnCl_2$, and 0.5 mM DTT). The beads were resuspended in 620 μl of buffer P and split into three aliquots of 200 μl. The beads were centrifuged, and the supernatant was removed to leave approximately 60 μl of total volume. One aliquot received recombinant Ptc1 (5.5 μg), the same amount of Ptc1 previously heated to 80° for 5 min, or the equivalent activity (measured using pNPP as substrate) of the recombinant yeast Ser/Thr phosphatase Ppz1 (2.1 μg). The mixtures were incubated for 90 min at 30°, and at the end of incubation, the samples were centrifuged and the supernatant removed. The beads were resuspended in sample buffer, boiled for 5 min, and subjected to SDS-PAGE. Radioactivity present in the gel was determined in a PMI System (BioRad).

Other techniques

Vacuole morphology was assessed by microscopic observation of FM4-64-treated cells as described previously (Vida and Emr 1995). Staining of bud scars for determination of budding pattern was performed in exponential cultures that were grown at 37° for 6–8 hr. Cells were fixed with 3.7% formaldehyde for 1 hr, washed with PBS, and stained with 0.02 mg/ml of CFW (Fluorescent Brightener F-6259; Sigma).

Reagent and data availability

Strains and constructs described in this paper are available on request.

Results

Screen for protein kinase mutants suppressing the ptc1 mutant defects

Cells lacking Ptc1 exhibit a variety of phenotypes that, directly or indirectly, are likely the result of hyperphosphorylation of certain, still unknown Ptc1 substrates. We considered that examination of the effect of deleting genes encoding nonessential kinases catalytic polypeptides and regulatory subunits might shed light on this question. To this end, we prepared a collection of double mutants combining the deletion of genes encoding 104 nonessential protein kinases, two lipid kinases (*FAB1* and *VPS34*), and nine regulatory subunits with that of *PTC1* by mean of transformation with deletion cassettes or by genetic crossing (see *Materials and Methods* for details).

The collection of strains then was tested for eight different known phenotypes derived from the *ptc1* mutation: increased sensitivity to LiCl, $CaCl_2$, $ZnCl_2$, CFW, caffeine, rapamycin, and high pH or inability to growth on ethanol as the only carbon source. A wide range of conditions (*i.e.*, cations and drug concentrations) was assayed, so it was possible to assign a score for each combination of mutations. Strains in which the mutation of the kinase did not alter the *ptc1* phenotype were scored as 0. Aggravation of the *ptc1* phenotype was observed only in a few cases, and these strains received a score of −1 or −2 based on the observed effect. Combinations in which the absence of the kinase improved growth for a given test condition were scored based on the potency of the effect from very mild (1) to very strong (7). The cumulative results for each phenotype are shown in

Table 2 Distribution of phenotypes for the double kinase-*ptc1* mutants for each specific test condition

	Test condition							
Effect	**$ZnCl_2$**	**CFW**	**Caffeine**	**$CaCl_2$**	**Rapamycin**	**Ethanol**	**pH**	**LiCl**
Negative	23	16	12	4	10	5	7	10
Neutral	72	80	54	27	16	33	13	24
Positive	20	19	49	84	89	77	95	81
Score 1–3	20	18	48	82	88	76	86	59
Score 4–7	0	1	1	2	1	1	9	22

Table 2. As can be seen, the sensitivity to Zn^{2+} ions and the cell-wall-damaging agent CFW were the phenotypes less frequently improved and more often worsened. In contrast, tolerance of the *ptc1* mutant to $CaCl_2$, rapamycin, high pH, and LiCl was improved by deletion of a substantial number of kinases. This effect was particularly relevant in the case of LiCl, for which 22 kinase deletions were able to substantially increase (scores 4–7) the tolerance to this toxic cation.

The score matrix also was used for clustering analysis. Figure 1 represents a heat map resulting from such analysis in which seven major clusters can be observed. Cluster 7 congregates the kinase mutations that result in worsening of the majority of the phenotypes. Both isoforms of the casein kinase 1 catalytic subunit (*YCK1* and *YCK2*) and one of the catalytic subunits of casein kinase 2 (*CKA2*) and its regulatory subunit (*CKB1*) are found in this cluster. Cluster 6 is composed of only two mutants, corresponding to *BCK1* and *SLT2*, which lack, respectively, the MAPKKK and the downstream MAPK of the CWI response pathway (Figure 1B). Remarkably, cluster 1 is composed of only one mutant lacking the *MKK1* gene, whose deletion results in a substantial improvement in all phenotypes tested. *MKK1* encodes one of the two MAPKKs upstream of Slt2, which are known to contribute to the signaling in response to cell-wall damage. It is worth noting that Mkk1 and Mkk2 have been considered for a long time to be redundant enzymes acting on Slt2. However, the *mkk2* mutant was included in cluster 3, indicating that this mutation cannot reproduce the effect of the deletion of *MKK1* in the *ptc1* background. This is better observed in Figure 1C, where the data corresponding to the genes involved in the three tiers of the CWI MAPK cascade are compared. To confirm this difference, we refined the phenotypic tests by directly comparing the tolerance of the wild-type strain, the *ptc1* mutant, the single *mkk1* and *mkk2* strains, and their combination with the *ptc1* mutation. As shown in Figure 2, individual mutation of neither *MKK1* nor *MKK2* affected growth in the conditions tested. Mutation of *MKK2* in the *ptc1* background moderately improved growth at high pH and in the presence of zinc ions but had little or no effect in modifying other phenotypes derived from the lack of Ptc1. In contrast, mutation of the *MKK1* isoform resulted in evident rescue of all tested *ptc1* phenotypes, leading in some cases, such as rapamycin and LiCl tolerance tests, to very robust growth. These results suggest that Mkk1 and Mkk2 necessarily could not be redundant enzymes and points to the CWI pathway, and specifically to Mkk1, as a possible major target for Ptc1 function.

Examination of the effect of the MKK1 and MKK2 deletions on diverse readouts related to ptc1 sensitivity phenotypes

To further confirm the differential effect of the *mkk1* and *mkk2* mutations in the suppression of the *ptc1* mutant defects and to gain additional information on the possible functions affected, we selected several readouts related to the Li^+, calcium, and rapamycin tolerance phenotypes.

The Na^+-ATPase-encoding gene *ENA1* is a key determinant of tolerance to toxic monovalent cations. Because the *ptc1* mutant shows decreased expression of *ENA1* in cells stressed with LiCl (Ruiz *et al.* 2006), we resorted to an *ENA1-lacZ* reporter (plasmid pKC201) to investigate the effect of the deletion of the kinases in the *ptc1* mutant. As observed in Figure 3A, mutation of *MKK1* significantly reversed ($P < 0.001$) the decrease in *ENA1* promoter activity observed in *ptc1* cells. However, deletion of *MKK2* had no effect. Because toxic cation tolerance of yeast cells strongly correlates with changes in the expression of *ENA1* (Arino *et al.* 2010), it is conceivable that partial restoration of normal *ENA1* function could explain the improvement in Li^+ tolerance observed in the double *mkk1 ptc1* mutant (Figure 2). In agreement with this notion, deletion of *MKK2* neither increases the activity of the *ENA1* promoter in *ptc1* cells nor improves tolerance to LiCl.

Lack of Ptc1 results in hyperactivation of calcineurin, and this can be demonstrated by monitoring the increase in expression from plasmid pAMS366, a *lacZ* reporter plasmid that carries a tandem of four calcineurin-dependent response elements (CDREs) from the calcineurin-regulatable *FKS2* promoter (Gonzalez *et al.* 2006). Figure 3B shows that deletion of *MKK1* in the *ptc1* background restored expression from pAMS366 to wild-type levels. In contrast, the activity of the synthetic promoter in the *ptc1 mkk2* strain was similar to that of the *ptc1* mutant, indicating that the impact on calcineurin caused by the absence of Ptc1 activity is neutralized specifically by the absence of *MKK1*. Remarkably, the increase in activity of the calcium-regulatable promoter caused by lack of Ptc1 was fully abolished not only by deletion of *CCH1* or *MID1*, encoding plasma membrane high-affinity calcium channels that are believed to work together, but also by deletion of *SLT2* (Figure 3B), suggesting a role for Slt2 in the activation of calcineurin triggered by the lack of Ptc1.

Inhibition of the TOR pathway by rapamycin resulted in induction of a number of genes that are subjected to nitrogen catabolite repression, such as *GAP1*, encoding a general amino acid permease, and *MEP1* and *MEP2*, encoding ammonium permeases. This induction is decreased in the *ptc1* mutant (Gonzalez *et al.* 2009) (Figure S1). We tested, by using transcriptional fusions of the promoters to the *lacZ* reporter gene, whether further deletion of *MKK1* or *MKK2*

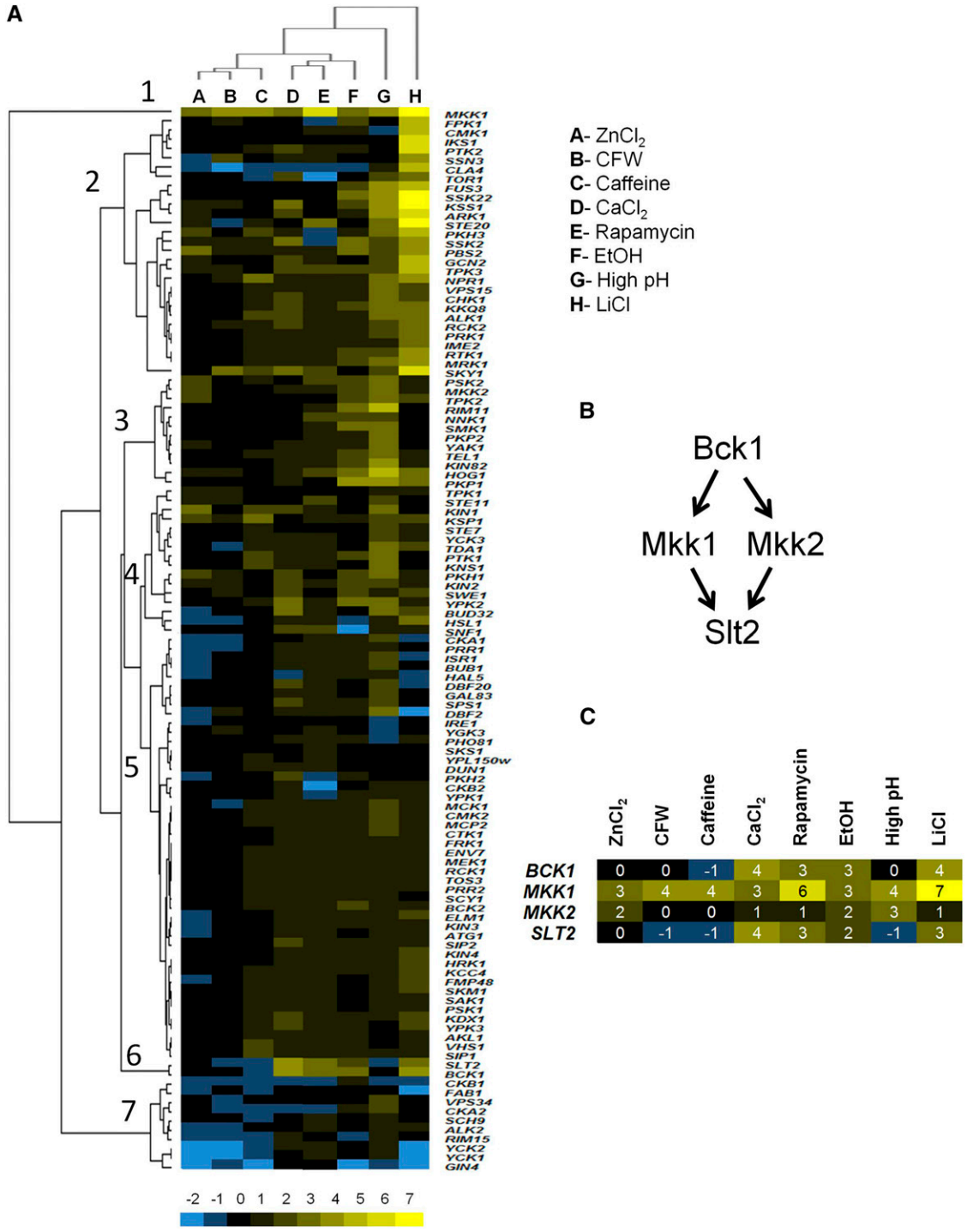

Figure 1 Phenotypic analysis of double *ptc1*-kinase gene mutants. Strains combining the deletion of 115 protein kinase catalytic or regulatory subunits encoding genes with that of *PTC1* were tested for the indicated phenotypes (A–H), and a score was assigned for each mutant-phenotype pair. (A) Clustering analysis was performed with cluster 3.0 (Euclidean distance, complete linkage) as represented with Java Treeview (Saldanha 2004). Zero score indicates that the mutation of the kinase does not alter the phenotype of the *ptc1* mutant; negative and positive scores denote worsening or improvement of growth under the specific condition, respectively. (B) Schema of the CWI MAPK module. (C) Inset showing the scores of kinases forming the three tiers of the CWI MAPK cascade.

would rescue normal gene expression. However, as seen in Figure S1, neither mutation of *MKK1* nor of *MKK2* restored normal levels of *GAP1*, *MEP1*, or *MEP2* promoter activity in the *ptc1* background on rapamycin treatment, thus suggesting that the positive effect of deletion of *MKK1* in *ptc1* cells when the TOR pathway is inhibited is not caused by the restoration of nitrogen catabolite repression signaling.

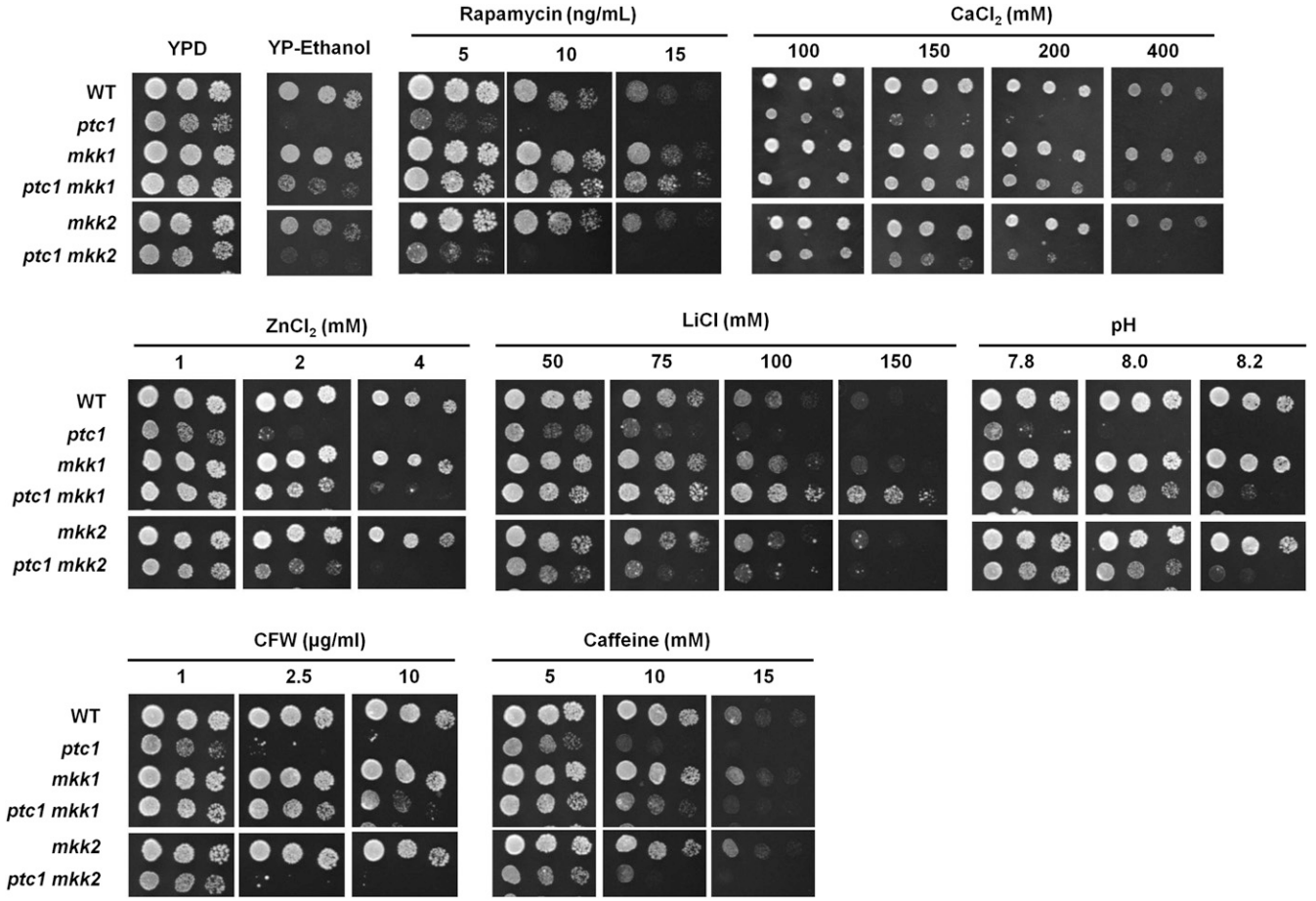

Figure 2 Comparative analysis of the effects of deletion of *MKK1* or *MKK2* in the *ptc1* background. Dilutions of the indicated mutants in the BY4741 background were spotted on YPD containing the indicated compounds, adjusted to different alkaline pH values, or on YP plates with ethanol as the sole carbon source. Photographs were taken after 72 hr of growth.

Removal of Mkk1 counteracts morphogenetic and vacuolar defects associated with lack of Ptc1 function

In addition to the phenotypic traits described earlier, lack of Ptc1 also provokes other deficiencies, such as cell separation defects, a random budding pattern in haploid cells at 37° (Gonzalez *et al.* 2006), and fragmented vacuoles (Bonangelino *et al.* 2002). We first investigated the effect of mutation of the Slt2 upstream kinases on the budding pattern of *ptc1* cells. To this end, cells were stained with CFW and examined by fluorescence microscopy. As shown in Figure 4A, lack of Mkk1 largely restored the normal budding pattern in *ptc1* cells, whereas mutation of *MKK2* had only a limited effect. Similarly, the cell-separation defect characteristic of the *ptc1* strains is substantially eliminated by deletion of *MKK1*, while the effect of mutation of *MKK2* was less marked (Figure 4B). We then examined the effect of the *MKK1* and *MKK2* deletions on the vacuolar phenotype of *ptc1* mutants. Vacuolar morphology was monitored in cells pretreated with the fluorescent lipophilic dye FM4-64. As shown in Figure 4C, deletion of *MKK1* largely normalized the vacuolar status in the *ptc1* mutant. In contrast, deletion of *MKK2* had no effect. We also included the *bck1 ptc1* and *slt2 ptc1* double mutants, lacking either the Bck1 kinase upstream Mkk1 and Mkk2 or their substrate, the Slt2 MAPK. Interestingly, in both cases, a perceptible improvement in vacuolar morphology could be observed. Collectively, all these experiments demonstrate that elimination of Mkk1 activity in cells deficient in Ptc1 function largely abolishes most of the phenotypic traits attributable to absence of the phosphatase.

Activation of the CWI pathway in ptc1 cells causes a delay in the G_2-M transition that is attenuated by removal of Mkk1

A parallel project in our laboratory in search of high-copy suppressors of the CFW sensitivity of *ptc1* cells (manuscript in preparation) identified, among others, several genes involved in promoting the G_2-M transition (such as *CLB1*, *MIH1*, and *PIN4*). Prompted by these results, we subjected nonsynchronized wild-type and *ptc1* cells to a low dose of CFW and monitored their DNA content by flow cytometry. As shown in Figure 4D, treatment with CFW did not affect wild-type cells but caused a marked accumulation of cells with replicated DNA in the *ptc1* strain, suggesting a delay in G_2-M transition. This delay was significantly suppressed

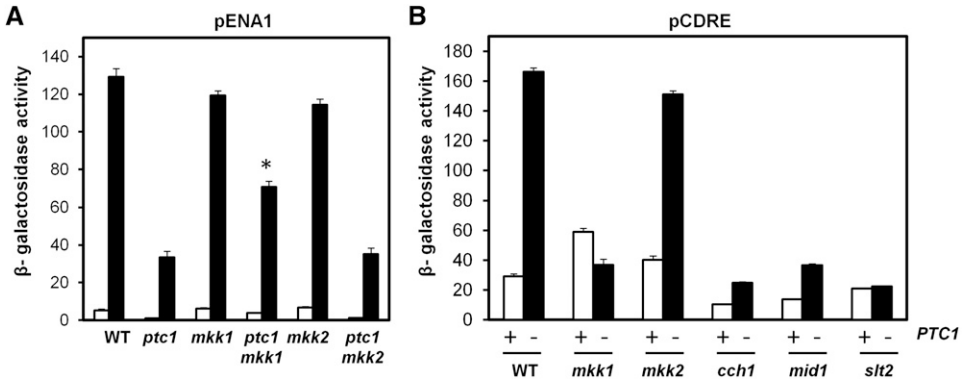

Figure 3 Deletion of *MKK1* normalizes decreased expression from the *ENA1* and calcineurin-regulatable promoters in *ptc1* mutants. (A) The indicated strains were transformed with plasmid pKC201 (pENA1) carrying a fusion of the *ENA1* promoter with the *lacZ* gene. Cells were stressed with 0.2 M LiCl for 1 hr (black bars), and β-galactosidase activity was measured. Data are mean ± SEM from at least 10 independent determinations. The asterisk denotes a statistically significant difference ($P < 0.001$) between *ptc1* and *ptc1 mkk1* strains. (B) Each *PTC1* (+) or *ptc1* (−) strain was deleted for the indicated genes. Cells were transformed with plasmid pAMS366 (pCDRE) containing four copies of a calcineurin-dependent response element (CDRE) from the *FKS2* promoter, and β-galactosidase activity was determined. Data are mean ± SEM from 6–14 experiments.

by additional deletion of *MKK1*, suggesting that hyperactivation of the CWI pathway in the *ptc1* mutant results in delayed G_2-M transition and that signaling through Mkk1 markedly contributes to this effect.

Ptc1 reduces CWI signaling by acting at the MAPKK level

The genetic experiments described so far point out to the Mkk1 kinase as a possible functional target for Ptc1. Our initial attempts to demonstrate that Ptc1 directly dephosphorylates Mkk1 were frustrated by the difficulty in purifying significant amounts of *in vivo* phosphorylated GST-fused Mkk1 from wild-type and *ptc1* cells (see later). Therefore, we further explored this possibility by epistatic analyses based on *PTC1* overexpression and using the dual phosphorylation of Slt2 as a readout of pathway activation. As occurred with Hog1 phosphorylation, overexpression of Ptc1, but not the adaptor protein Nbp2, reduced the amount of phosphorylated Slt2 (Figure 5A) both in the absence and in the presence of Congo red, a compound that interferes with chitin organization, leading to CWI pathway stimulation (Marin *et al.* 2009). In contrast, overexpression of Ptc1 did not decrease the level of phospho-Fus3 and phospho-Kss1 of pheromone-stimulated cells (data not shown), indicating that Ptc1 overexpression does not result in indiscriminate nonspecific downregulation of MAPK signaling. To activate the CWI pathway at the level of the MAPK module, we used a constitutively active version of the MAPKKK Bck1 that lacks the first 1171 amino acids ($Bck1^{CT}$) (Sacristan-Reviriego *et al.* 2015). As shown in Figure 5B, overexpression of Ptc1 was able to reduce the strong Slt2 phosphorylation promoted by $Bck1^{CT}$. Because this version does not contain the N-terminal Nbp2-binding proline-rich motif (Hruby *et al.* 2011), we previously confirmed that Nbp2 is not necessary for overexpressed Ptc1 to act on the CWI pathway (Figure S2). $Bck1^{CT}$ also lacks the phosphorylation sites necessary for its activation by Pkc1 (Levin *et al.* 1994). Therefore, Ptc1 does not decrease Slt2 phosphorylation by promoting the dephosphorylation of Bck1. Moreover, the fact that GST-Ptc1 overexpression still reduced the Slt2 phosphorylation promoted by $Bck1^{CT}$ in a *pkc1* strain (Figure 5C) clearly shows that the target is neither Pkc1 nor Bck1 but a downstream kinase.

We next addressed whether Ptc1 acts at the level of the MAPK, as described previously for the HOG pathway (Warmka *et al.* 2001). As shown in Figure 5D, overproduction of Ptc1 did not reduce Slt2 phosphorylation in a *bck1* strain expressing a constitutively active Mkk1-mutated version ($MKK1^{S386P}$) (Watanabe *et al.* 1995). This clearly shows that Ptc1 is not able to directly dephosphorylate the MAPK Slt2. Together these results provide genetic evidence that Ptc1 impinges on the CWI pathway at the MAPKK level.

To clarify which MAPKK is the Ptc1 target, we used *mkk1* and *mkk2* mutant cells. Overexpression of Ptc1 reduced Slt2 phosphorylation in both mutant strains when the pathway was activated either by expressing constitutively active upstream components of the pathway, such as $Bck1^{CT}$ (Figure 5E), Bck1-20 (Lee and Levin 1992), and $PKC1^{R398A,R405A,K406A}$ (Figure S3, A and B) or by heat stress (Martin *et al.*, 2000) (Figure S3C). These data indicate that despite the different pattern of genetic interactions between *PTC1* and *MKK1* or *MKK2* shown earlier, Ptc1 is able to downregulate both CWI MAPKKs.

Mkk1, but not Mkk2, is required for the increased CWI signaling displayed by ptc1Δ mutants

Experiments shown in Figure 5E and Figure S3 also provided evidence that the *mkk1*Δ mutant displays a lower level of Slt2 phosphorylation than *mkk2*Δ cells in all tested conditions. The same pattern also was observed under several cell-wall stresses (Figure S4A). The different phospho-Slt2 levels showed by *mkk1* and *mkk2* mutants correlate with their distinct Rlm1-mediated gene expression, as determined by using the CWI transcriptional reporter *MLP1-LacZ* (Garcia *et al.*, 2009) (Figure S4B).

Moreover, the lack of Mkk1, but not that of Mkk2, promoted a strong reduction of the high level of Slt2 phosphorylation displayed by the *ptc1* mutant (Figure 6A). This effect was observed both in the absence and in the presence of Congo red, and it was specific for the CWI pathway because removal of neither Mkk1 nor Mkk2 showed significant influence on the increased Hog1 phosphorylation displayed by *ptc1* mutant cells (Figure 6A). Consistently, in a *ptc1* mutant

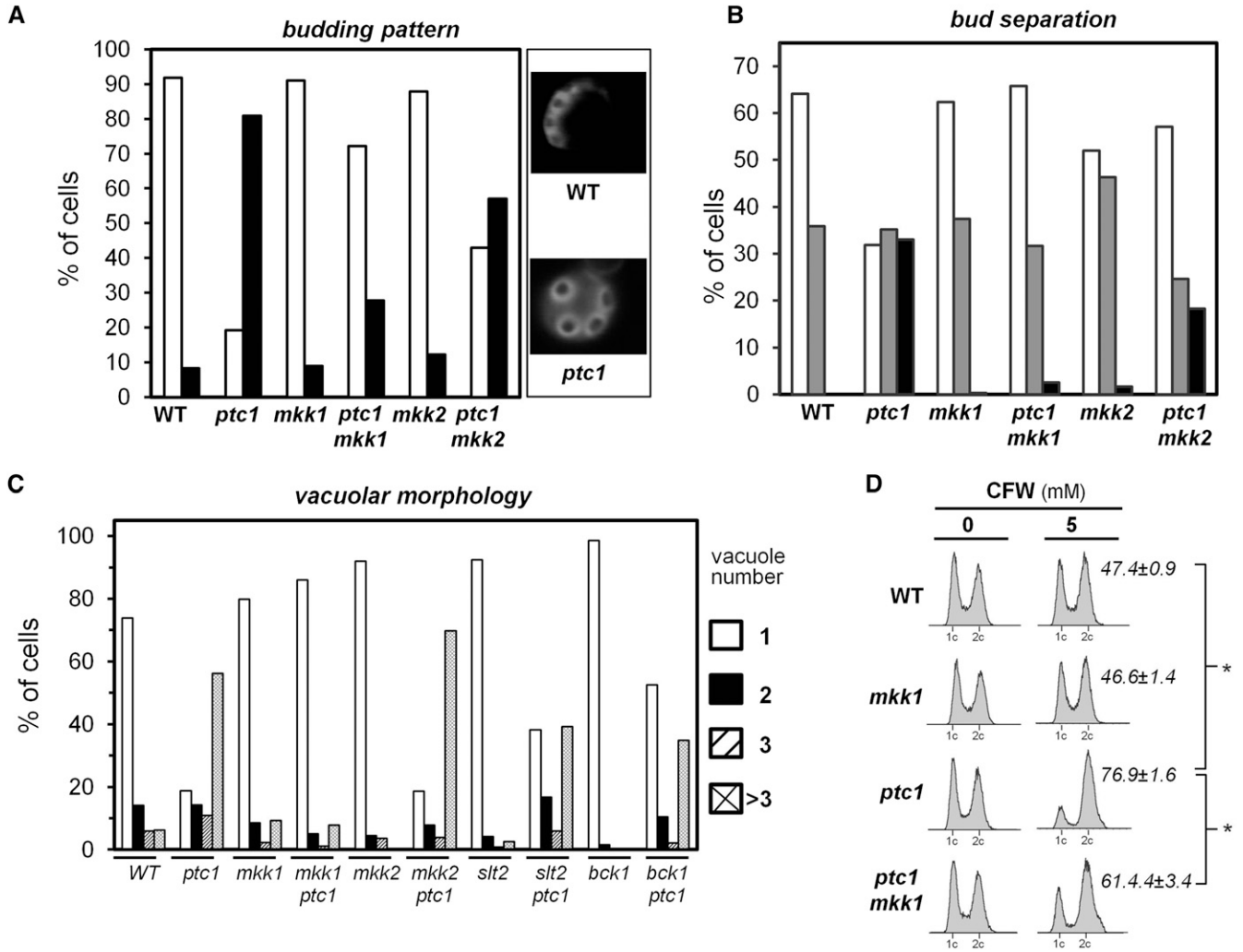

Figure 4 Suppression of additional *ptc1*-related phenotypes by deletion of *MKK1*. (A) Budding pattern. Cultures of the indicated strains were grown at 37° and stained with CFW to visualize bud scars. The budding pattern was examined (at least 250 cells), and the percentage of normal (white bars) or random haploid budding (black bars) was determined. The inset shows typical (wild type) or random (*ptc1*) patterns (×600). (B) Bud separation. Cultures were prepared as in A, except that no staining was performed. Cultures were slightly sonicated, and samples were examined for number of buds in each cell. Three categories were defined: unbudded cells (white bars), cells containing one bud (gray bars), and cells containing more than one bud (black bars). The percentage corresponding to each category is represented. At least 750 cells were examined for each strain. (C) Vacuolar morphology. The indicated strains were incubated with fluorescent dye FM4-64 to visualize vacuole morphology. At least 150 cells for each strain were classified into four different classes (1, 2, 3, or >3 vacuoles/cell), and the frequency was plotted as percentage over the total number of cells. (D) Cell-cycle delay. Exponentially growing cultures of the indicated strains were treated for 2 hr with 5 mM CFW (or vehicle) and processed for propidium iodide staining and flow cytometry to monitor DNA content. Numbers on the right indicate the percentage of cells at G_2 (see *Materials and Methods*) for the CFW treatment and represent the mean ± SD from five samples obtained in three independent experiments. Asterisks denote that the difference between means is statistically significant ($P < 0.005$).

transformed with the CWI transcriptional reporter *MLP1-GFP* (Rodriguez-Peña *et al.*, 2008), only the deletion of *MKK1* reduced GFP fluorescence to similar levels as those displayed by wild-type cells both in the absence and in the presence of Congo red (Figure 6B). All these results indicate that phosphorylation of Slt2 and consequent activation of the CWI transcriptional response are mainly mediated by Mkk1. Furthermore, expression of the wild-type but not a kinase-dead version of this MAPKK in the *mkk1 ptc1* double mutant restored the high Slt2 phosphorylation level characteristic of the single *ptc1* mutant (Figure 6C). Because the abundance of inactive Mkk1 is even higher than that of the wild-type protein, it can be concluded that the ability of Mkk1 to maintain a high Slt2 activation in *ptc1* mutant cells depends on its kinase activity.

Further evidence of the major role of Mkk1 for signaling through the CWI pathway and of the influence of Ptc1 in this process was obtained by expressing a GST-Slt2 fusion version in wild-type, *ptc1*, *mkk1*, and *ptc1 mkk1* double-mutant strains and shifting the cultures to high pH (8.2), which rapidly activates the CWI pathway and induces phosphorylation of Slt2 (Serrano *et al.* 2006). GST-Slt2 was isolated by affinity

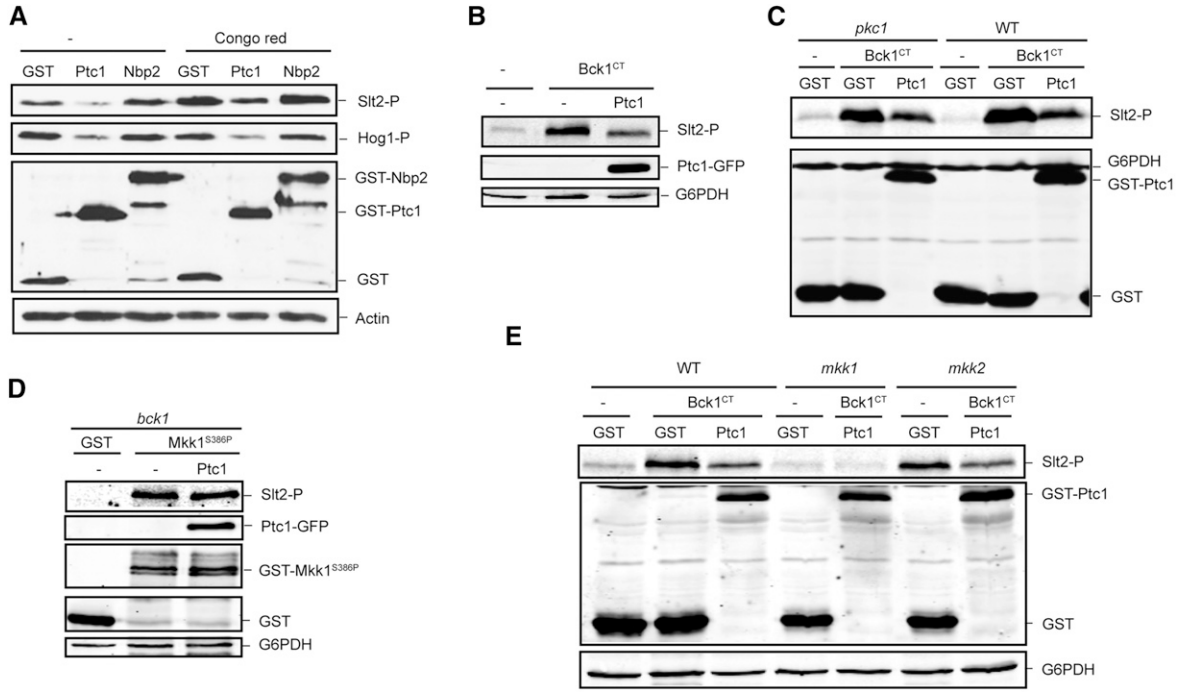

Figure 5 Ptc1 acts on the CWI pathway at the level of the MAPKKs. (A) Western blotting analysis in the wild-type strain BY4741 transformed with pEG(KG) (GST), pEG(KG)-PTC1, or pEG(KG)-NBP2. Cells were grown to mid-log phase in raffinose-based medium, then galactose was added to a final concentration of 2% for 2 hr, and cells were treated or not (−) with Congo red (30 μg/ml) for additional 2 hr. Phospho-Slt2, phospho-Hog1, GST-fused proteins, and actin (loading control) were detected with anti-phospho-p42/44, anti-phospho-p38, anti-GST, and anti-actin antibodies, respectively. (B) Western blotting analysis performed as in A in the wild-type strain YPH499 transformed with YCplG (−) or YCplG-PTC1-GFP and pYES3 (−) or pYES3-BCK1^{CT}, as indicated. Ptc1-GFP was detected with anti-GFP and G6PDH (as loading control) with anti-G6PDH antibodies. (C) Western blotting analysis performed as in A in the wild-type strain CML128 and the isogenic *pkc1* mutant transformed with pEG-(KG) (GST) or pEG (KG)-PTC1 and pYES3 (−) or pYES3-BCK1^{CT}. Cells were grown as in A but in medium with 0.8 M sorbitol. (D) Western blotting analysis performed as in A of the *bck1* strain Y01328 transformed with plasmids YCplG (−) or YCplG-PTC1-GFP and pEG(KG) (GST) or pEG-(KG)-MKK1^{S386P}, as indicated. (E) Western blotting analysis performed as in A in the wild-type strain YPH499 and the isogenic *mkk1* and *mkk2* mutants transformed with pEG-(KG) (GST) or pEG(KG)-PTC1 and pYES3 (−) or pYES3-*BCK1^{CT}*.

chromatography, the samples were resolved by SDS-PAGE and stained, and the excised bands were subjected to tryptic digestion. After enrichment for phosphopeptides, samples were analyzed by MS, the peptide containing the phosphorylatable Thr and Tyr at the activation loop was identified, and the ratio of phosphorylated to total peptide was calculated. We found that the phosphorylation level of this peptide was 5.6-fold higher in *ptc1* than in *mkk1* cells and that deletion of *MKK1* in the *ptc1* mutant resulted in reduction of the phosphorylation levels to that of the single *mkk1* mutant (Figure S5). These data further confirm that in the absence of Ptc1, Slt2 results in hyperactivation in response to stress in a way that essentially depends on Mkk1 function.

Together our results fit with the notion that the sensitivity of *ptc1* mutants to cell-wall-altering agents is mostly due to hyperactivity of the CWI pathway, which is strongly reduced in the absence of Mkk1 (Figure 2 and Figure S3C), and reinforces the idea that Mkk1 is more effective than Mkk2 in signaling to Slt2

The apparent difference in protein abundance between the native and kinase-dead versions of Mkk1 in a *ptc1* background observed in the experiment shown in Figure 6C suggested that cells might be downregulating the level of Mkk1 as a response to the inability to inactivate the kinase by dephosphorylation. To test this possibility, wild-type, *ptc1*, *slt2*, and *ptc1 slt2* cells were transformed with either centromeric or high-copy plasmids bearing epitope-tagged native Mkk1 or its equivalent kinase-dead (K250R) version. As shown in Figure 6D, when the native version of the Mkk1 kinase was expressed from a centromeric plasmid in *ptc1* cells, the amount of this kinase was markedly lower than in the wild-type strain, whereas further deletion of Slt2 restored Mkk1 wild-type levels. Interestingly, the amount of Mkk1 protein did not decrease in the *ptc1* background when the form devoid of kinase activity was expressed. It is important to note that, in contrast, the level of Mkk2 in the absence of Ptc1 was similar in either its active or inactive forms (Figure 6C). The effect of deletion of *SLT2* on Mkk1 levels was particularly dramatic when *MKK1* was expressed from a high-copy-number vector (Figure 6D). These results point to the idea that in the absence of Ptc1 and as a response to the subsequent hyperactivation of Slt2, the cell attempts to avoid an exacerbated level of Mkk1 kinase activity by decreasing the amount of Mkk1 protein.

Ptc1 dephosphorylates in vitro GST-Mkk1

The results described earlier could be explained if Ptc1 were acting directly on Mkk1 by dephosphorylating and

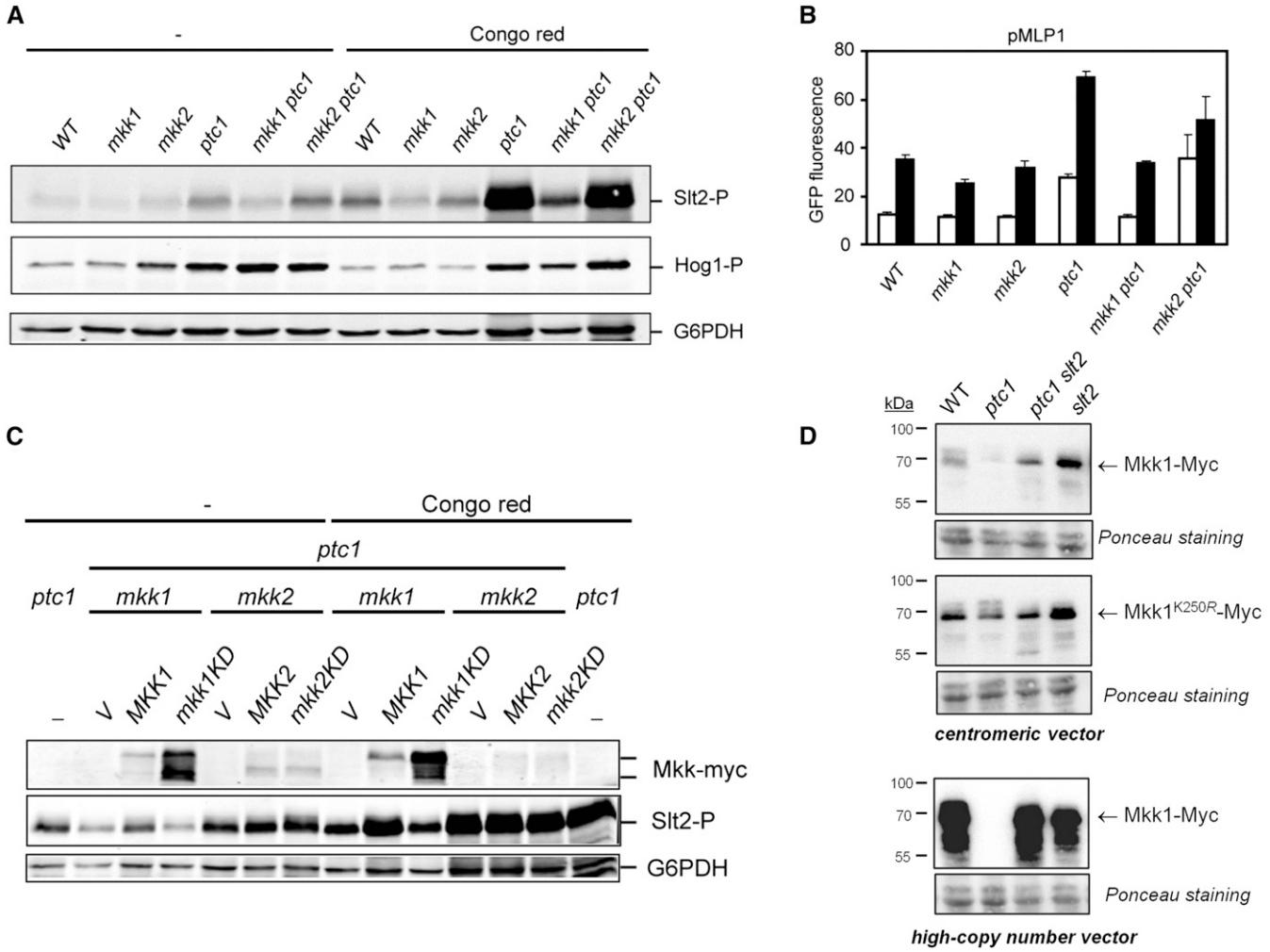

Figure 6 Mkk1 kinase activity is essential for *ptc1* mutants to display high Slt2 activation. (A) Western blotting analysis in the wild-type strain BY4741 and the indicated isogenic mutants. Exponentially growing cells at 24° in YPD were treated or not (−) with Congo red (30 μg/ml) for 3 hr. Phospho-Slt2, phospho-Hog1, and G6PDH (loading control) were detected with anti-phospho-p42/44, anti-phospho-p38, and anti-G6PDH antibodies, respectively. (B) Expression of *MLP1-GFP* determined by flow cytometry in the same growth conditions and strains as in A but carrying the plasmid pMLP1-GFP. Data are mean ± SD from three independent transformants. (C) Western blotting analysis performed as in A in the indicated mutant strains transformed with the empty vector pRS416 (V) or plasmids pRS416-MKK1myc, pRS416-MKK1^{K250R}myc (*MKK1KD*), pRS416-MKK2myc, or pRS416-MKK2^{K243R}myc (*MKK2KD*). Mkk1 and Mkk2 were detected with anti-myc antibodies. (D) The indicated strains were transformed with plasmid pRS416-MKK1myc or pRS416-MKK1^{K250R}myc (centromeric vector) or YEp352-MKK1myc (high-copy-number vector), and the amount of expressed Mkk1 was monitored by Western blot analysis. Ponceau staining is included for loading and transfer reference.

inactivating this MAPKK. To test this possibility, we expressed in *E. coli* Mkk1 fused to GST and purified the protein by means of glutathione agarose beads. Recombinant Mkk1 bound to the beads was phosphorylated *in vitro* with ^{32}P-labeled ATP using a yeast extract from a strain overexpressing the hyperactive Bck1-20 allele as a source of kinase activity to increase the amount of phosphorylated Mkk1. This strain also lacks Slt2 to avoid the retrophosphorylation of Mkk1 exerted by this MAPK in residues different from the conserved activation sites phosphorylated by Bck1 (Jimenez-Sanchez *et al.* 2007). Phosphorylated GST-Mkk1 was then incubated with either recombinant Ptc1, the same amount of heat-inactivated Ptc1, or Ppz1, a PP1-like Ser/Thr protein phosphatase that has been genetically related to (Lee *et al.* 1993; Posas *et al.* 1993) but is not directly involved in the CWI pathway (Merchan *et al.* 2004). As can be seen in Figure 7, after treatment with heat-inactivated Ptc1 or active Ppz1, Mkk1 appears radioactively labeled to a similar amount. In contrast, treatment with active Ptc1 results in the disappearance of most of the radioactive phosphate previously incorporated into the protein. This indicates that Ptc1 recognizes Mkk1 as a substrate and shows that this is not a common feature for yeast Ser/Thr PPases.

Discussion

Ptc1 is known to be involved in a wide variety of cellular processes, but most cellular targets for its phosphatase

activity are unknown. The high number of genetic interactions of *PTC1* with protein kinase genes found in our work confirms the functional broadness of this protein phosphatase. Remarkably, only the mutation of Mkk1, one of the MAPKKs of the CWI pathway, was able to substantially suppress all the phenotypes of the *ptc1* mutant tested in the screen (Figure 1 and Figure 2), as well as additional defects attributable to the *ptc1* mutation (Figure 3 and Figure 4). This finding reinforces previous evidence linking Ptc1 to the CWI pathway (Huang and Symington 1995; Gonzalez *et al.* 2006; Hruby *et al.* 2011; Stanger *et al.* 2012; Sacristan-Reviriego *et al.* 2015) and strongly suggests that abnormal activation of the CWI pathway is at the basis of many of the defects derived from the absence of Ptc1. It must be noted that an excessive activation of the CWI pathway can be deleterious, as observed when hyperactive alleles of Pkc1 or Mkk1 are overexpressed (Watanabe *et al.* 1995; Martin *et al.* 2000). Based on this finding, it would be expected that deletion of components upstream (*BCK1*) or downstream (*SLT2*) of Mkk1 in the CWI MAPK module also would attenuate the *ptc1* phenotypes. However, this is not the case for the sensitivity to CFW, caffeine, or high pH because the compensatory response mediated by the CWI pathway itself is essential for cell viability under cell-wall-damaging conditions. The different effect of the *MKK1* deletion would be attributable to the existence of another MAPKK, Mkk2, whose residual activity is able to sufficiently activate Slt2 to cope with cell-wall stress conditions but not to convey a deleterious hyperactivation of the CWI pathway. This fits with the heat map presented in Figure 1, in which *BCK1* and *SLT2* cluster together, but distant from *MKK1*.

The results presented here strongly support the idea that Mkk1 conveys most of the signaling flow through the pathway, as deduced from the observations that (1) elimination of Mkk1 but not Mkk2 attenuates a large variety of *ptc1* defects, (2) lack of Mkk1 gives rise to a great reduction in both Slt2 phosphorylation and its derived transcriptional response, which is not observed in the *mkk2* strain, and (3) cells lacking Ptc1 avoid accumulation of the native version of Mkk1 but tolerate the inactive version of the kinase, and elimination of Slt2 restores wild-type Mkk1 protein levels. This evidence confirms initial studies suggesting that Mkk1 could be a stronger Slt2 activator than Mkk2 (Martin *et al.* 2000). The preeminent role of Mkk1 over Mkk2 cannot be attributed to a higher abundance of Mkk1 because evaluation of the data collected at the PaxDb (Wang *et al.* 2015) indicates that, in most studies, Mkk2 cellular protein levels are found to be similar to or even higher than those of Mkk1. Therefore, alternative possibilities must be considered (*i.e.*, different specific activity or distinct subcellular localization). In any case, the major role of Mkk1 as activating the CWI pathway is observed under all conditions tested, and therefore, it is likely based on intrinsic functional properties of this MAPKK and not dependent on mechanisms operating under specific stimuli.

Our results support a model in which many cellular phenotypes described for the *ptc1* mutant could be attributable to an anomalous activation of the Slt2 pathway derived from

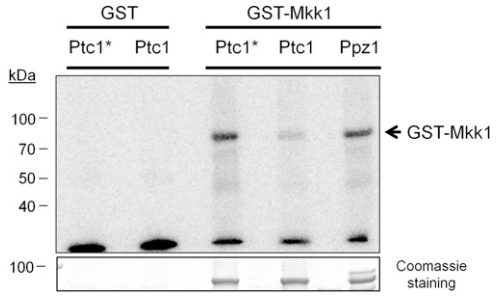

Figure 7 Ptc1 dephosphorylates Mkk1 *in vitro*. Recombinant GST-Mkk1 bound to glutathione agarose beads was incubated with yeast extract obtained from *slt2* cells expressing the hyperactive allele Bck1–20 in the presence of [γ-^{32}P]ATP. After extensive washing, phosphorylated Mkk1 was incubated with equivalent amounts of heat-inactivated Ptc1 (Ptc1*), active Ptc1, or Ppz1. The beads were resuspended in sample buffer and boiled, and the supernatant was subjected to 8% SDS-PAGE. Radioactivity was detected by means of a PMI system (BioRad). Recombinant GST was also included in the experiment as a control. Coomassie staining of the relevant section of the gel shows the amount of GST-Mkk1 present in the different lanes.

the incapacity to properly dephosphorylate and downregulate Mkk1. For instance, activation of the CWI pathway by eliminating Msg5, the major Slt2 phosphatase, also results in increased sensitivity to cell-wall stress (Flandez *et al.* 2004). Moreover, the cortical ER inheritance defect displayed by *ptc1* cells is suppressed by either loss of Slt2 or inhibition of the CWI pathway (Du *et al.* 2006; Li *et al.* 2013). In addition, Ptc1-dependent inactivation of Slt2 is also needed for mitochondrial inheritance (Li *et al.* 2010), suggesting that hyperactivation of this pathway is at the basis of these defects. Our findings also emphasize the multiple regulatory roles of the CWI pathway and stress the importance of an appropriate negative modulation of this route for cellular homeostasis. An example would be the impact of Ptc1 on calcium homeostasis. We reported that a major effect derived from the lack of Ptc1 was a calcineurin-mediated increase in sensitivity to calcium ions and an increased expression of calcineurin-dependent genes (Gonzalez *et al.* 2006), and it is shown here that these effects are largely abolished by deletion of *MKK1* (Figure 2 and Figure 3B). We propose that the impact of the lack of Ptc1 on calcium homeostasis is the result of hyperactivation of the Slt2 pathway. It can be conceived that augmented Slt2 pathway activity would result in increased entry of calcium ions from the medium. This notion is sustained by (1) the early observation that Slt2 activation is required for calcium entry through the cell membrane Mid1 and Cch1 transporters (Bonilla and Cunningham 2003), (2) the recent evidence that a *ptp2 msg5* phosphatase double mutant, which has an increased level of activated Slt2, is also highly sensitive to calcium in a calcineurin-dependent fashion (Lavina *et al.* 2013), and (3) our own finding that removal of either Slt2 or the calcium plasma membrane transporters eliminates activation of a calcium-regulatable reporter displayed by *ptc1* cells (Figure 3B). It is also known that deletion of both *PTP2* and *MSG5* causes vacuolar fragmentation (Hermansyah *et al.*

2009), as the *ptc1* mutation does, suggesting that this also might be caused by Slt2 hyperactivation. Because the yeast vacuole is the major reservoir for intracellular calcium, vacuolar fragmentation could exacerbate the effect of enhanced calcium entry. However, vacuolar fragmentation caused by the *ptc1* mutation simply could be a physiologic response to the enhanced entry of calcium, leading to improved sequestration of the cation at the vacuole by maximizing its surface-volume ratio (Kane 2006) because this phenotype also has been observed in mutants with constitutive high levels of cytosolic calcium (Kellermayer *et al.* 2003).

The genetic and biochemical analyses presented in Figure 5 indicate that Ptc1 acts at the level of the MAPKK tier of the CWI MAPK module. We also provide evidence that Ptc1 can dephosphorylate *in vitro* recombinant Mkk1 previously phosphorylated by a yeast extract prepared from cells with an activated CWI pathway. This evidence, together with the large number of specific genetic interactions observed between *PTC1* and *MKK1*, allows us to postulate that Ptc1 is likely a major Mkk1 phosphatase *in vivo*. Note, however, that whereas our data also suggest that Ptc1 is able to dephosphorylate Mkk2, the limited influence of this MAPKK in CWI signaling would explain the scarce relevance of such negative regulation. Protein phosphatases are the main negative regulators of MAPK pathways, and so far, all the known phosphatases acting on yeast MAPK modules dephosphorylate the MAPK (Martin *et al.* 2005). For instance, in the HOG pathway, Ptc1 is recruited to the MAPKK Pbs2 through the adaptor Nbp2 to act on the MAPK Hog1 (Mapes and Ota 2004). In contrast, in the CWI pathway, Ptc1 would be recruited by Nbp2 to the MAPKKK Bck1 to dephosphorylate the MAPKKs. Therefore, our results highlight the ability of this protein phosphatase to dephosphorylate a variety of elements of MAPK pathways in yeast, as occurs in mammals, where PP2C phosphatases negatively regulate the three different components of the MAPK signaling module (Lammers and Lavi 2007).

Acknowledgments

We thank Victor J. Cid for providing plasmids and advice. We acknowledge Montserrat Robledo for technical assistance and the Unidad de Genómica (UCM) for DNA sequencing. This work was supported by grants BFU2011-30197-C3-01 and BFU2014-54591-C2-1-P to J.A. and BIO2010-22369-C02-01 and BIO2013-44112-P to M.M. (Ministry of Science and Innovation and Ministry of Economy and Competitivity, Spain and FEDER) and S2011/BMD-2414 from Comunidad Autónoma de Madrid (Spain) to M.M. J.A. was recipient of an "Ajut 2014-SGR-4" (Generalitat de Catalunya) and an ICREA Academia 2009 Award (Generalitat de Catalunya). L.T., A.S.-R., and L.P. were supported by predoctoral fellowships from the Ministry of Science and Innovation and the Ministry of Education (Spain).

Author contributions: L.T. constructed diverse strains and expression plasmids and performed the screens, most phenotypic analyses, and the *lacZ* assays. C.C. generated most of the kinase phosphatase deletion strains and contributed to the initial phenotypic analyses. A.G. and B.R.-P. contributed to the phenotypic analyses. A.S.-R. carried out most Western blotting analyses and some phenotypic analyses and *lacZ* assays. L.P. generated strains and carried out initial Western blotting analyses. D.C. contributed to the Mkk1 dephosphorylation assays. A.S.-C. performed the cell-cycle assays by flow cytometry. H.M., M.M., and J.A. designed the experiments, supervised the work, discussed the results, and wrote the paper.

Literature Cited

Adams, A., D. E. Gottschling, C. A. Kaiser, and T. Stearns, 1997 *Methods in Yeast Genetics*. Cold Spring Harbor Laboratory Press, Cold Spring Harbor, NY.

Alepuz, P. M., K. W. Cunningham, and F. Estruch, 1997 Glucose repression affects ion homeostasis in yeast through the regulation of the stress-activated ENA1 gene. Mol. Microbiol. 26: 91–98.

Andrés-Pons, A., I. Rodríguez-Escudero, A. Gil, A. Blanco, A. Vega *et al.*, 2007 In vivo functional analysis of the counterbalance of hyperactive phosphatidylinositol 3-kinase p110 catalytic oncoproteins by the tumor suppressor PTEN. Cancer Res. 67: 9731–9739.

Arino, J., J. Ramos, and H. Sychrova, 2010 Alkali metal cation transport and homeostasis in yeasts. Microbiol. Mol. Biol. Rev. 74: 95–120.

Arino, J., A. Casamayor, and A. Gonzalez, 2011 Type 2C protein phosphatases in fungi. Eukaryot. Cell 10: 21–33.

Barreto, L., D. Canadell, S. Petrezselyova, C. Navarrete, L. Maresova *et al.*, 2011 A genomewide screen for tolerance to cationic drugs reveals genes important for potassium homeostasis in Saccharomyces cerevisiae. Eukaryot. Cell 10: 1241–1250.

Bermejo, C., E. Rodriguez, R. Garcia, J. M. Rodriguez-Pena, M. L. Rodriguez de la Concepcion *et al.*, 2008 The sequential activation of the yeast HOG and SLT2 pathways is required for cell survival to cell wall stress. Mol. Biol. Cell 19: 1113–1124.

Bonangelino, C. J., E. M. Chavez, and J. S. Bonifacino, 2002 Genomic screen for vacuolar protein sorting genes in *Saccharomyces cerevisiae*. Mol. Biol. Cell 13: 2486–2501.

Bonilla, M., and K. W. Cunningham, 2003 Mitogen-activated protein kinase stimulation of Ca^{2+} signaling is required for survival of endoplasmic reticulum stress in yeast. Mol. Biol. Cell 14: 4296–4305.

Brachmann, C. B., A. Davies, G. J. Cost, E. Caputo, J. Li *et al.*, 1998 Designer deletion strains derived from Saccharomyces cerevisiae S288C: a useful set of strains and plasmids for PCR-mediated gene disruption and other applications. Yeast 14: 115–132.

de la Torre-Ruiz, A., J. Torres, J. Arino, and E. Herrero, 2002 Sit4 is required for proper modulation of the biological functions mediated by Pkc1 and the cell integrity pathway in *Saccharomyces cerevisiae*. J. Biol. Chem. 277: 33468–33476.

Du, Y., L. Walker, P. Novick, and S. Ferro-Novick, 2006 Ptc1p regulates cortical ER inheritance via Slt2p. EMBO J. 25: 4413–4422.

Flandez, M., I. C. Cosano, C. Nombela, H. Martin, and M. Molina, 2004 Reciprocal regulation between Slt2 MAPK and isoforms of Msg5 dual-specificity protein photophatase modulates the yeast cell integrity pathway. J. Biol. Chem. 279: 11027–11034.

Garcia, R., J. M. Rodriguez-Peña, C. Bermejo, C. Nombela, and J. Arroyo, 2009 The high osmotic response and cell wall integrity pathways cooperate to regulate transcriptional responses to zymolyase-induced cell wall stress in *Saccharomyces cerevisiae*. J. Biol. Chem. 284: 10901–10911.

Garcia-Gimeno, M. A., I. Munoz, J. Arino, and P. Sanz, 2003 Molecular characterization of Ypi1, a novel *Saccharomyces cerevisiae* type 1 protein phosphatase inhibitor. J. Biol. Chem. 278: 47744–47752.

Gonzalez, A., A. Ruiz, R. Serrano, J. Arino, and A. Casamayor, 2006 Transcriptional profiling of the protein phosphatase 2C family in yeast provides insights into the unique functional roles of Ptc1. J. Biol. Chem. 281: 35057–35069.

Gonzalez, A., A. Ruiz, A. Casamayor, and J. Arino, 2009 Normal function of the yeast TOR pathway requires the type 2C protein phosphatase Ptc1. Mol. Cell. Biol. 29: 2876–2888.

Hahn, J. S., and D. J. Thiele, 2002 Regulation of the Saccharomyces cerevisiae Slt2 kinase pathway by the stress-inducible Sdp1 dual specificity phosphatase. J. Biol. Chem. 277: 21278–21284.

Hermansyah, M., Y. Sugiyama, Kaneko, and S. Harashima, 2009 Yeast protein phosphatases Ptp2p and Msg5p are involved in G_1-S transition, CLN2 transcription, and vacuole morphogenesis. Arch. Microbiol. 191: 721–733.

Hruby, A., M. Zapatka, S. Heucke, L. Rieger, Y. Wu *et al.*, 2011 A constraint network of interactions: protein-protein interaction analysis of the yeast type II phosphatase Ptc1p and its adaptor protein Nbp2p. J. Cell Sci. 124: 35–46.

Huang, K. N., and L. S. Symington, 1995 Suppressors of a Saccharomyces cerevisiae pkc1 mutation identify alleles of the phosphatase gene PTC1 and of a novel gene encoding a putative basic leucine zipper protein. Genetics 141: 1275–1285.

Ito, T., T. Chiba, R. Ozawa, M. Yoshida, M. Hattori *et al.*, 2001 A comprehensive two-hybrid analysis to explore the yeast protein interactome. Proc. Natl. Acad. Sci. USA 98: 4569–4574.

Jimenez-Sanchez, M., V. J. Cid, and M. Molina, 2007 Retrophosphorylation of Mkk1 and Mkk2 MAPKKs by the Slt2 MAPK in the yeast cell integrity pathway. J. Biol. Chem. 282: 31174–31185.

Jin, Y., E. P. Taylor, F. Tang, and L. S. Weisman, 2009 PTC1 is required for vacuole inheritance and promotes the association of the myosin-V vacuole-specific receptor complex. Mol. Biol. Cell 20: 1312–1323.

Kane, P. M., 2006 The where, when, and how of organelle acidification by the yeast vacuolar H^+-ATPase. Microbiol. Mol. Biol. Rev. 70: 177–191.

Kellermayer, R., D. P. Aiello, A. Miseta, and D. M. Bedwell, 2003 Extracellular Ca(2+) sensing contributes to excess Ca (2+) accumulation and vacuolar fragmentation in a pmr1Delta mutant of S. cerevisiae. J. Cell Sci. 116: 1637–1646.

Lammers, T., and S. Lavi, 2007 Role of type 2C protein phosphatases in growth regulation and in cellular stress signaling. Crit. Rev. Biochem. Mol. Biol. 42: 437–461.

Lavina, W. A., M. Hermansyah, Y. Sugiyama, Kaneko, and S. Harashima, 2013 Functionally redundant protein phosphatase genes PTP2 and MSG5 co-regulate the calcium signaling pathway in Saccharomyces cerevisiae upon exposure to high extracellular calcium concentration. J. Biosci. Bioeng. 115: 138–146.

Le Guezennec, X., and D. V. Bulavin, 2010 WIP1 phosphatase at the crossroads of cancer and aging. Trends Biochem. Sci. 35: 109–114.

Lee, K. S., and D. E. Levin, 1992 Dominant mutations in a gene encoding a putative protein kinase (BCK1) bypass the requirement for a Saccharomyces cerevisiae protein kinase C homolog. Mol. Cell. Biol. 12: 172–182.

Lee, K. S., L. K. Hines, and D. E. Levin, 1993 A pair of functionally redundant yeast genes (PPZ1 and PPZ2) encoding type 1-related protein phosphatases function within the PKC1-mediated pathway. Mol. Cell. Biol. 13: 5843–5853.

Lesage, G., A. M. Sdicu, P. Menard, J. Shapiro, S. Hussein *et al.*, 2004 Analysis of beta-1,3-glucan assembly in Saccharomyces cerevisiae using a synthetic interaction network and altered sensitivity to caspofungin. Genetics 167: 35–49.

Levin, D. E., 2011 Regulation of cell wall biogenesis in Saccharomyces cerevisiae: the cell wall integrity signaling pathway. Genetics 189: 1145–1175.

Levin, D. E., B. Bowers, C. Y. Chen, Y. Kamada, and M. Watanabe, 1994 Dissecting the protein kinase C/MAP kinase signalling pathway of Saccharomyces cerevisiae. Cell. Mol. Biol. Res. 40: 229–239.

Li, X., Y. Du, S. Siegel, S. Ferro-Novick, and P. Novick, 2010 Activation of the mitogen-activated protein kinase, Slt2p, at bud tips blocks a late stage of endoplasmic reticulum inheritance in Saccharomyces cerevisiae. Mol. Biol. Cell 21: 1772–1782.

Li, X., S. Ferro-Novick, and P. Novick, 2013 Different polarisome components play distinct roles in Slt2p-regulated cortical ER inheritance in Saccharomyces cerevisiae. Mol. Biol. Cell 24: 3145–3154.

Maeda, T., A. Y. Tsai, and H. Saito, 1993 Mutations in a protein tyrosine phosphatase gene (PTP2) and a protein serine/threonine phosphatase gene (PTC1) cause a synthetic growth defect in Saccharomyces cerevisiae. Mol. Cell. Biol. 13: 5408–5417.

Maeda, T., S. M. Wurgler-Murphy, and H. Saito, 1994 A two-component system that regulates an osmosensing MAP kinase cascade in yeast. Nature 369: 242–245.

Mapes, J., and I. M. Ota, 2004 Nbp2 targets the Ptc1-type 2C Ser/Thr phosphatase to the HOG MAPK pathway. EMBO J. 23: 302–311.

Marin, M. J., M. Flandez, C. Bermejo, J. Arroyo, H. Martin *et al.*, 2009 Different modulation of the outputs of yeast MAPK-mediated pathways by distinct stimuli and isoforms of the dual-specificity phosphatase Msg5. Mol. Genet. Genomics 281: 345–359.

Marini, A. M., S. Soussi-Boudekou, S. Vissers, and B. Andre, 1997 A family of ammonium transporters in Saccharomyces cerevisiae. Mol. Cell. Biol. 17: 4282–4293.

Markovich, S., A. Yekutiel, I. Shalit, Y. Shadkchan, and N. Osherov, 2004 Genomic approach to identification of mutations affecting caspofungin susceptibility in Saccharomyces cerevisiae. Antimicrob. Agents Chemother. 48: 3871–3876.

Martin, H., J. M. Rodriguez-Pachon, C. Ruiz, C. Nombela, and M. Molina, 2000 Regulatory mechanisms for modulation of signaling through the cell integrity Slt2-mediated pathway in *Saccharomyces cerevisiae*. J. Biol. Chem. 275: 1511–1519.

Martin, H., M. Flandez, C. Nombela, and M. Molina, 2005 Protein phosphatases in MAPK signalling: we keep learning from yeast. Mol. Microbiol. 58: 6–16.

Merchan, S., D. Bernal, R. Serrano, and L. Yenush, 2004 Response of the *Saccharomyces cerevisiae* Mpk1 mitogen-activated protein kinase pathway to increases in internal turgor pressure caused by loss of Ppz protein phosphatases. Eukaryot. Cell 3: 100–107.

Mitchell, D. A., T. K. Marshall, and R. J. Deschenes, 1993 Vectors for the inducible overexpression of glutathione S-transferase fusion proteins in yeast. Yeast 9: 715–722.

Parsons, A. B., R. L. Brost, H. Ding, Z. Li, C. Zhang *et al.*, 2004 Integration of chemical-genetic and genetic interaction data links bioactive compounds to cellular target pathways. Nat. Biotechnol. 22: 62–69.

Posas, F., A. Casamayor, and J. Arino, 1993 The PPZ protein phosphatases are involved in the maintenance of osmotic stability of yeast cells. FEBS Lett. 318: 282–286.

Ram, A. F., A. Wolters, H. R. Ten, and F. M. Klis, 1994 A new approach for isolating cell wall mutants in Saccharomyces cerevisiae by screening for hypersensitivity to calcofluor white. Yeast 10: 1019–1030.

Reynolds, A., V. Lundblad, D. Dorris, and M. Keaveney, 1997 Yeast vectors and assays for expression of cloned genes, pp. 13.6.1–13.6.6 in *Current Protocols in Molecular Biology*, edited by F. M. Ausubel, R. Brent, R. E. Kingston, D. D. Moore, and J. G. Seidman *et al*. Wiley, New York.

Robinson, M. K., W. H. van Zyl, E. M. Phizicky, and J. R. Broach, 1994 *TPD1* of *Saccharomyces cerevisiae* encodes a protein phosphatase 2C-like activity implicated in tRNA splicing and cell separation. Mol. Cell. Biol. 14: 3634–3645.

Rodriguez-Escudero, I., R. Rotger, V. J. Cid, and M. Molina, 2006 Inhibition of Cdc42-dependent signalling in Saccharomyces cerevisiae by phosphatase-dead SigD/SopB from Salmonella typhimurium. Microbiology 152: 3437–3452.

Rodriguez-Peña, J. M., S. Díez-Muniz, C. Nombela, and J. Arroyo, 2008 A yeast strain biosensor to detect cell wall-perturbing agents. J. Biotechnol. 133: 311–317.

Roeder, A. D., G. J. Hermann, B. R. Keegan, S. A. Thatcher, and J. M. Shaw, 1998 Mitochondrial inheritance is delayed in *Saccharomyces cerevisiae* cells lacking the serine/threonine phosphatase PTC1. Mol. Biol. Cell 9: 917–930.

Ruiz, A., A. González, R. García-Salcedo, J. Ramos, and J. Arino, 2006 Role of protein phosphatases 2C on tolerance to lithium toxicity in the yeast *Saccharomyces cerevisiae*. Mol. Microbiol. 62: 263–277.

Ruiz, A., X. Xu, and M. Carlson, 2013 Ptc1 protein phosphatase 2C contributes to glucose regulation of SNF1/AMP-activated protein kinase (AMPK) in Saccharomyces cerevisiae. J. Biol. Chem. 288: 31052–31058.

Sacristan-Reviriego, A., H. Martin, and M. Molina, 2015 Identification of putative negative regulators of yeast signaling through a screening for protein phosphatases acting on cell wall integrity and mating MAPK pathways. Fungal Genet. Biol. 77: 1–11.

Saldanha, A. J., 2004 Java Treeview—extensible visualization of microarray data. Bioinformatics 20: 3246–3248.

Sambade, M., M. Alba, A. M. Smardon, R. W. West, and P. M. Kane, 2005 A genomic screen for yeast vacuolar membrane ATPase mutants. Genetics 170: 1539–1551.

Seeley, E. S., M. Kato, N. Margolis, W. Wickner, and G. Eitzen, 2002 Genomic analysis of homotypic vacuole fusion. Mol. Biol. Cell 13: 782–794.

Serrano, R., D. Bernal, E. Simon, and J. Arino, 2004 Copper and iron are the limiting factors for growth of the yeast Saccharomyces cerevisiae in an alkaline environment. J. Biol. Chem. 279: 19698–19704.

Serrano, R., H. Martin, A. Casamayor, and J. Arino, 2006 Signaling alkaline pH stress in the yeast Saccharomyces cerevisiae through the Wsc1 cell surface sensor and the Slt2 MAPK pathway. J. Biol. Chem. 281: 39785–39795.

Sharmin, D., Y. Sasano, M. Sugiyama, and S. Harashima, 2014 Effects of deletion of different PP2C protein phosphatase genes on stress responses in Saccharomyces cerevisiae. Yeast 31: 393–409.

Stanger, K., M. Gorelik, and A. R. Davidson, 2012 Yeast adaptor protein, Nbp2p, is conserved regulator of fungal Ptc1p phosphatases and is involved in multiple signaling pathways. J. Biol. Chem. 287: 22133–22141.

Stathopoulos, A. M., and M. S. Cyert, 1997 Calcineurin acts through the CRZ1/TCN1-encoded transcription factor to regulate gene expression in yeast. Genes Dev. 11: 3432–3444.

Uetz, P., L. Giot, G. Cagney, T. A. Mansfield, R. S. Judson *et al.*, 2000 A comprehensive analysis of protein-protein interactions in Saccharomyces cerevisiae. Nature 403: 623–627.

Vida, T. A., and S. D. Emr, 1995 A new vital stain for visualizing vacuolar membrane dynamics and endocytosis in yeast. J. Cell Biol. 128: 779–792.

Wang, M., C. J. Herrmann, M. Simonovic, D. Szklarczyk, and C. von Mering, 2015 Version 4.0 of PaxDb: protein abundance data, integrated across model organisms, tissues, and cell-lines. Proteomics 15: 3163–3168.

Warmka, J., J. Hanneman, J. Lee, D. Amin, and I. Ota, 2001 Ptc1, a type 2C Ser/Thr phosphatase, inactivates the HOG pathway by dephosphorylating the mitogen-activated protein kinase Hog1. Mol. Cell. Biol. 21: 51–60.

Watanabe, Y., K. Irie, and K. Matsumoto, 1995 Yeast RLM1 encodes a serum response factor-like protein that may function downstream of the Mpk1 (Slt2) mitogen-activated protein kinase pathway. Mol. Cell. Biol. 15: 5740–5749.

Winzeler, E. A., D. D. Shoemaker, A. Astromoff, H. Liang, K. Anderson *et al.*, 1999 Functional characterization of the S. cerevisiae genome by gene deletion and parallel analysis. Science 285: 901–906.

Xie, M. W., F. Jin, H. Hwang, S. Hwang, V. Anand *et al.*, 2005 Insights into TOR function and rapamycin response: chemical genomic profiling by using a high-density cell array method. Proc. Natl. Acad. Sci. USA 102: 7215–7220.

Zhu, H., J. F. Klemic, S. Chang, P. Bertone, A. Casamayor *et al.*, 2000 Analysis of yeast protein kinases using protein chips. Nat. Genet. 26: 283–289.

Zhu, Y. H., and D. V. Bulavin, 2012 Wip1-dependent signaling pathways in health and diseases. Prog. Mol. Biol. Transl. Sci. 106: 307–325.

Communicating editor: D. J. Lew

GENETICS

Supporting Information
www.genetics.org/lookup/suppl/doi:10.1534/genetics.115.183202/-/DC1

Wide-Ranging Effects of the Yeast Ptc1 Protein Phosphatase Acting Through the MAPK Kinase Mkk1

Laura Tatjer, Almudena Sacristán-Reviriego, Carlos Casado, Asier González, Boris Rodríguez-Porrata, Lorena Palacios, David Canadell, Albert Serra-Cardona, Humberto Martín, María Molina, and Joaquín Ariño

DOI: 10.1534/genetics.115.183202

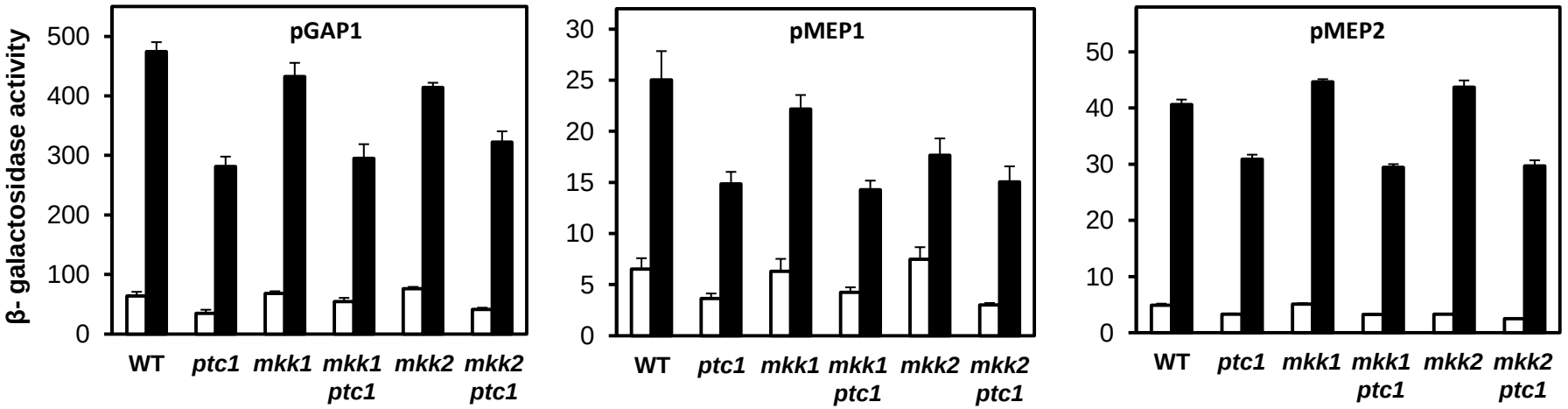

FIGURE S1. Mutation of *MKK1* or *MKK2* does not rescue deficient expression of NCR-regulated genes in the *ptc1* mutant. The indicated strains were transformed with *lacZ* reporter plasmids for several NCR-regulated genes: *GAP1* (pGAP1), *MEP1* (pMEP1), and *MEP2* (pMEP2). Cells were treated with vehicle (open bars) or 200 ng/ml rapamycin (closed bars) for 60 min (pGAP1) or 90 min (pMEP1 and pMEP2) and β-galactosidase activity measured. Data are mean ± SEM. from 6 to 10 experiments.

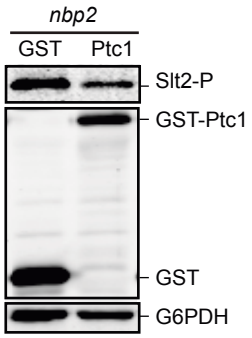

Figure S2: Nbp2 is not necessary for overexpressed Ptc1 to reduce signaling trough the CWI patway. Western blotting analysis of cell wall extracts from the *nbp2*Δ strain Y03520 transformed with pEG(KG) (GST) or pEG(KG)-PTC1 (Ptc1). Cells were grown to mid-log phase in raffinose-based medium, then galactose was added to a final 2% for 2 h. Phospho-Slt2, GST-fused proteins, and G6PDH (loading control) were detected with anti-phospho-p42/44, anti-GST and anti-G6PDH antibodies, respectively.

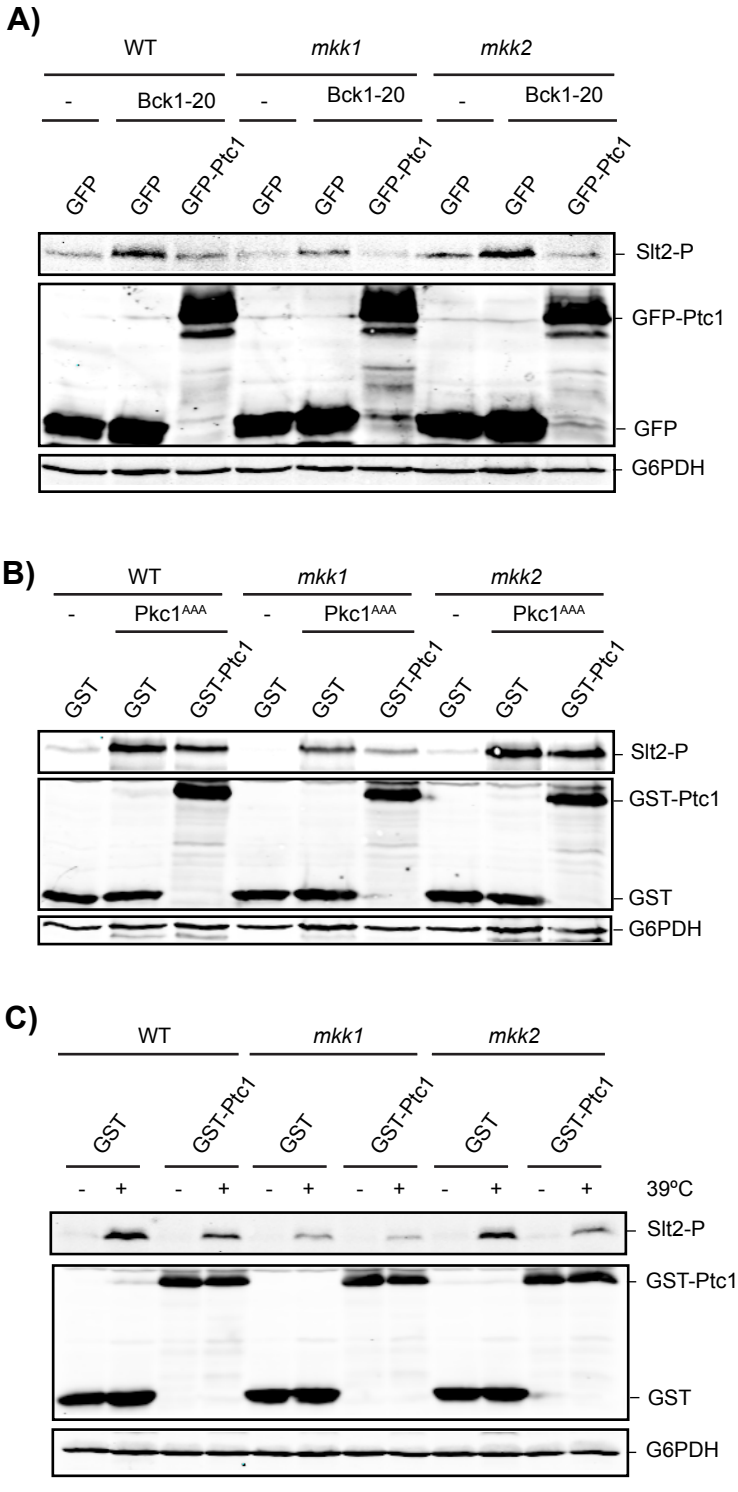

Figure S3: Ptc1 acts on both Mkk1 and Mkk2. A) Western blotting analysis of cell extracts from the wild type strain YPH499 and the isogenic *mkk1*Δ and *mkk2*Δ strains transformed with pYES3-GFP or pYES3-GFP-PTC1 and pRS316 or pRS316-BCK1-20. Cells were grown to mid-log phase in raffinose-based medium, then galactose was added to a final 2% for 2 h. Phospho-Slt2, GFP-fused proteins, and G6PDH (loading control) were detected with anti-phospho-p42/44, anti-GFP and anti-G6PDH antibodies, respectively. **B)** Western blotting analysis in the same strains as in A, transformed with plasmids transformed with pEG-(KG) or pEG(KG)-PTC1 and YCplac112 (-) or YCplac112-PKC1^{AAA}. **C)** Western blotting in the wild type strain BY4741 and the isogenic *mkk1*Δ and *mkk2*Δ strains, transformed with pEG-(KG) or pEG(KG)-PTC1. Cells were cultured at 24ºC (-) or at 39 ºC (+) for one hour.

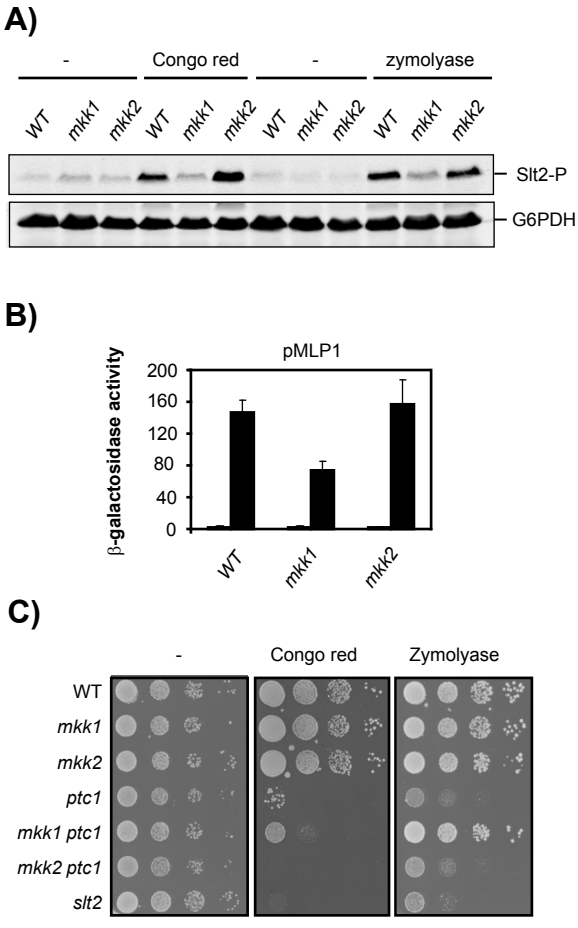

Figure S4: Mkk1 is the main MAPKK involved in signal transmission through the CWI pathway in response to Congo Red and zymolyase
A) Western blotting analysis performed as in Figure 6 in WT strain BY4741 and the isogenic *mkk1*Δ and *mkk2*Δ mutants. Exponentially growing cells at 24 °C in YPD were treated or not with Congo red (30µg/ml) or zymolyase 100T (0.8 U/ml) for 3 h. **B)** Expression of *MLP1*-LacZ was determined as β-galactosidase activity in cells of the same strains as in A, but carrying the plasmid p-MLP1-LacZ, grown in the absence (white bars) or the presence (black bars) of Congo Red. Data are mean ± SD from three independent experiments in triplicate. **C)** 10-fold dilution series of the wild type strain BY4741 and the indicated isogenic mutants were spotted on YPD and YPD containing Congo Red (75µg/ml) or zymolyase 20T (200 µg/ml). Plates were incubated at 24ºC and growth was monitored after 48 h.

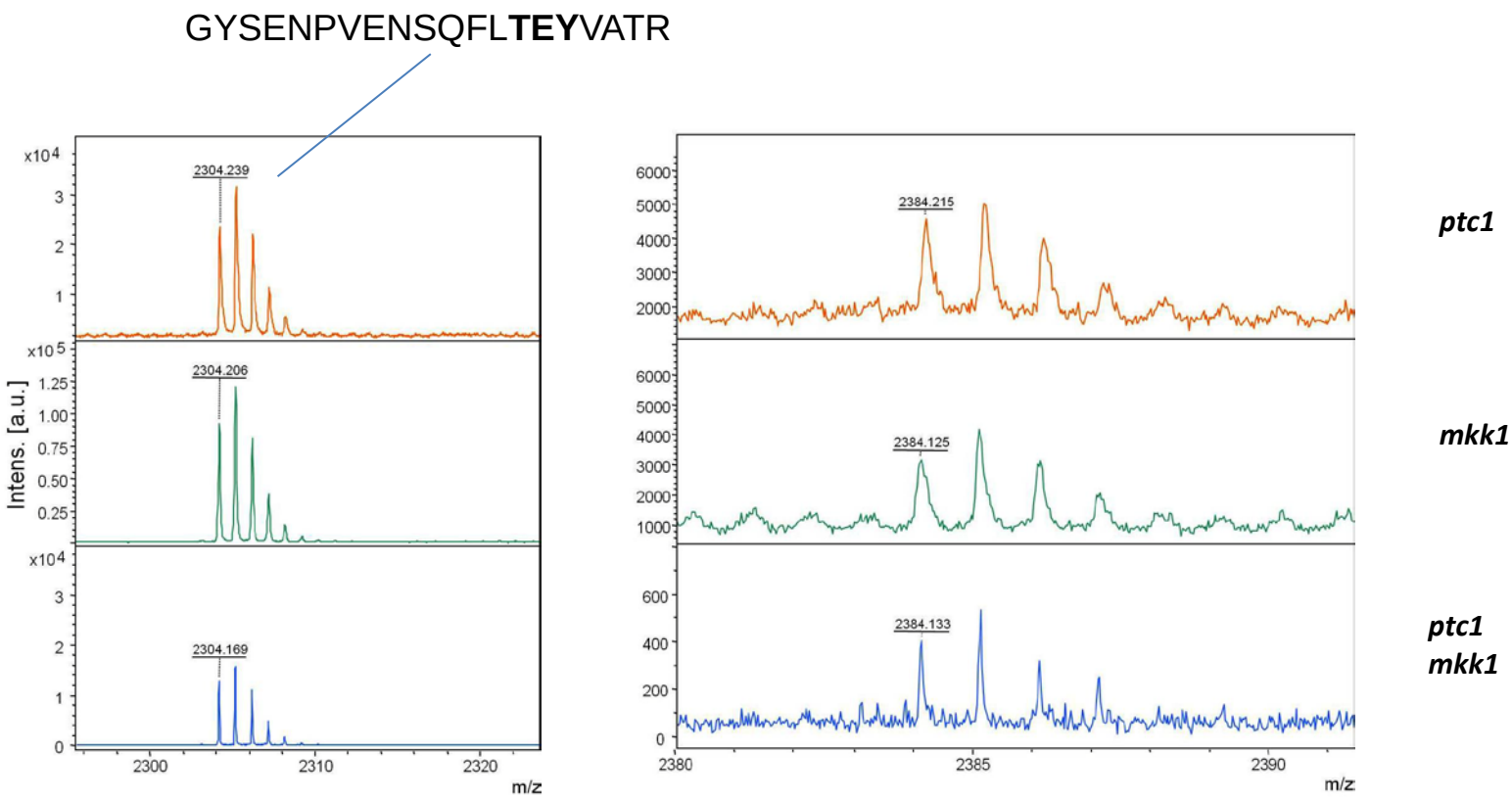

Figure S5. MS profile of unphosphorylated (left) and phosphorylated (right) peptide containing the Slt2 activating phosphorylatable residues. The calculated phospho/unphosphorylated ratios were 19.4 (*ptc1*), 3.4 (*mkk1*) and 3.1 *(ptc1 mkk1*).

Table S1. Strains used in the screen (RSA, Random Spore analysis; TA, Tetrad Analysis)

			Strains employed		
Name	**Genotype**	**Construction Method**	**Haploid Strain MAT a**	**Haploid Strain MAT α (BY4741)**	**Double mutant Background**
CCV61	***psk1::kanMX4 ptc1::nat1***	RSA	MAR216 (BY4742 *ptc1::nat1*)	*psk1::kanMX4*	BY4741
CCV62	***kin3::kanMX4 ptc1::nat1***	RSA	MAR216 (BY4742 *ptc1::nat1*)	*kin3::kanMX4*	BY4741
CCV63	***alk2::kanMX4 ptc1::nat1***	RSA	MAR216 (BY4742 *ptc1::nat1*)	*alk2::kanMX4*	BY4741
CCV65	***tel1::kanMX4 ptc1::nat1***	RSA	MAR216 (BY4742 *ptc1::nat1*)	*tel1::kanMX4*	BY4741
CCV67	***akl1::kanMX4 ptc1::nat1***	RSA	MAR216 (BY4742 *ptc1::nat1*)	*akl1::kanMX4*	BY4741
CCV72	***kin82::kanMX4 ptc1::nat1***	RSA	MAR216 (BY4742 *ptc1::nat1*)	*kin82::kanMX4*	BY4741
CCV73	***rtk1::kanMX4 ptc1::nat1***	RSA	MAR216 (BY4742 *ptc1::nat1*)	*rtk1::kanMX4*	BY4741
CCV74	***mrk1::kanMX4 ptc1::nat1***	RSA	MAR216 (BY4742 *ptc1::nat1*)	*mrk1::kanMX4*	BY4741
CCV75	***dun1::kanMX4 ptc1::nat1***	RSA	MAR216 (BY4742 *ptc1::nat1*)	*dun1::kanMX4*	BY4741
CCV79	***vhs1::kanMX4 ptc1::nat1***	RSA	MAR216 (BY4742 *ptc1::nat1*)	*vhs1::kanMX4*	BY4741
CCV81	***sip1::kanMX4 ptc1::nat1***	RSA	MAR216 (BY4742 *ptc1::nat1*)	*sip1::kanMX4*	BY4741
CCV85	***gin4::kanMX4 ptc1::nat1***	RSA	MAR216 (BY4742 *ptc1::nat1*)	*gin4::kanMX4*	BY4741
CCV86	***sps1::kanMX4 ptc1::nat1***	RSA	MAR216 (BY4742 *ptc1::nat1*)	*sps1::kanMX4*	BY4741
CCV87	***gal83::kanMX4 ptc1::nat1***	RSA	MAR216 (BY4742 *ptc1::nat1*)	*gal83::kanMX4*	BY4741
CCV88	***yck3::kanMX4 ptc1::nat1***	RSA	MAR216 (BY4742 *ptc1::nat1*)	*yck3::kanMX4*	BY4741
CCV89	***sak1::kanMX4 ptc1::nat1***	RSA	MAR216 (BY4742 *ptc1::nat1*)	*sak1::kanMX4*	BY4741
CCV90	***bck2::kanMX4 ptc1::nat1***	RSA	MAR216 (BY4742 *ptc1::nat1*)	*bck2::kanMX4*	BY4741
CCV94	***alk1::kanMX4 ptc1::nat1***	RSA	MAR216 (BY4742 *ptc1::nat1*)	*alk1::kanMX4*	BY4741
CCV96	***rck1::kanMX4 ptc1::nat1***	RSA	MAR216 (BY4742 *ptc1::nat1*)	*rck1::kanMX4*	BY4741
CCV97	***tos3::kanMX4 ptc1::nat1***	RSA	MAR216 (BY4742 *ptc1::nat1*)	*tos3::kanMX4*	BY4741
CCV98	***atg1::kanMX4 ptc1::nat1***	RSA	MAR216 (BY4742 *ptc1::nat1*)	*atg1::kanMX4*	BY4741
CCV102	***dbf2::kanMX4 ptc1::nat1***	RSA	MAR216 (BY4742 *ptc1::nat1*)	*dbf2::kanMX4*	BY4741
CCV103	***bub1::kanMX4 ptc1::nat1***	RSA	MAR216 (BY4742 *ptc1::nat1*)	*bub1::kanMX4*	BY4741
CCV104	***pho81::kanMX4 ptc1::nat1***	RSA	MAR216 (BY4742 *ptc1::nat1*)	*pho81::kanMX4*	BY4741
CCV105	***bud32::kanMX4 ptc1::nat1***	RSA	MAR216 (BY4742 *ptc1::nat1*)	*bud32::kanMX4*	BY4741
CCV113	***pkp1::kanMX4 ptc1::nat1***	RSA	MAR216 (BY4742 *ptc1::nat1*)	*pkp1::kanMX4*	BY4741
CCV117	***ime2::kanMX4 ptc1::nat1***	RSA	MAR216 (BY4742 *ptc1::nat1*)	*ime2::kanMX4*	BY4741
CCV118	***pbs2::kanMX4 ptc1::nat1***	RSA	MAR216 (BY4742 *ptc1::nat1*)	*pbs2::kanMX4*	BY4741

CCV122	***swe1::kanMX4 ptc1::nat1***	RSA	MAR216 (BY4742 *ptc1::nat1*)	*swe1::kanMX4*	BY4741
CCV123	***ptk2::kanMX4 ptc1::nat1***	RSA	MAR216 (BY4742 *ptc1::nat1*)	*ptk2::kanMX4*	BY4741
CCV127	***prr1::kanMX4 ptc1::nat1***	RSA	MAR216 (BY4742 *ptc1::nat1*)	*prr1::kanMX4*	BY4741
CCV128	***ypk1::kanMX4 ptc1::nat1***	RSA	MAR216 (BY4742 *ptc1::nat1*)	*ypk1::kanMX4*	BY4741
CCV130	***kdx1::kanMX4 ptc1::nat1***	RSA	MAR216 (BY4742 *ptc1::nat1*)	*kdx1::kanMX4*	BY4741
CCV132	***kkq8::kanMX4 ptc1::nat1***	RSA	MAR216 (BY4742 *ptc1::nat1*)	*kkq8::kanMX4*	BY4741
CCV135	***kns1::kanMX4 ptc1::nat1***	RSA	MAR216 (BY4742 *ptc1::nat1*)	*kns1::kanMX4*	BY4741
CCV139	***rck2::kanMX4 ptc1::nat1***	RSA	MAR216 (BY4742 *ptc1::nat1*)	*rck2::kanMX4*	BY4741
CCV142	***ypk2::kanMX4 ptc1::nat1***	RSA	MAR216 (BY4742 *ptc1::nat1*)	*ypk2::kanMX4*	BY4741
CCV145	***tda1::kanMX4 ptc1::nat1***	RSA	MAR216 (BY4742 *ptc1::nat1*)	*tda1::kanMX4*	BY4741
CCV147	***yck2::kanMX4 ptc1::nat1***	RSA	MAR216 (BY4742 *ptc1::nat1*)	*yck2::kanMX4*	BY4741
CCV153	***cmk2::kanMX4 ptc1::nat1***	RSA	MAR216 (BY4742 *ptc1::nat1*)	*cmk2::kanMX4*	BY4741
CCV156	***skm1::kanMX4 ptc1::nat1***	RSA	MAR216 (BY4742 *ptc1::nat1*)	*skm1::kanMX4*	BY4741
CCV160	***kin4::kanMX4 ptc1::nat1***	RSA	MAR216 (BY4742 *ptc1::nat1*)	*kin4::kanMX4*	BY4741
CCV161	***hrk1::kanMX4 ptc1::nat1***	RSA	MAR216 (BY4742 *ptc1::nat1*)	*hrk1::kanMX4*	BY4741
LTR012	***gcn2::kanMX4 ptc1::nat1***	TA	MAR216 (BY4742 *ptc1::nat1*)	*gcn2::kanMX4*	BY4741
LTR013	***yak1::kanMX4 ptc1::nat1***	TA	MAR216 (BY4742 *ptc1::nat1*)	*yak1::kanMX4*	BY4741
LTR015	***cka2::kanMX4 ptc1::nat1***	TA	MAR216 (BY4742 *ptc1::nat1*)	*cka2::kanMX4*	BY4741
LTR016	***kin2::kanMX4 ptc1::nat1***	TA	MAR216 (BY4742 *ptc1::nat1*)	*kin2::kanMX4*	BY4741
LTR017	***tpk2::kanMX4 ptc1::nat1***	TA	MAR216 (BY4742 *ptc1::nat1*)	*tpk2::kanMX4*	BY4741
LTR032	***psk2::kanMX4 ptc1::nat1***	TA	MAR216 (BY4742 *ptc1::nat1*)	*psk2::kanMX4*	BY4741
LTR033	***ckb2::kanMX4 ptc1::nat1***	TA	MAR216 (BY4742 *ptc1::nat1*)	*ckb2::kanMX4*	BY4741
LTR034	***kss1::kanMX4 ptc1::nat1***	TA	MAR216 (BY4742 *ptc1::nat1*)	*kss1::kanMX4*	BY4741
LTR035	***ark1::kanMX4 ptc1::nat1***	TA	MAR216 (BY4742 *ptc1::nat1*)	*ark1::kanMX4*	BY4741
LTR040	***kin1::kanMX4 ptc1::nat1***	TA	MAR216 (BY4742 *ptc1::nat1*)	*kin1::kanMX4*	BY4741
LTR041	***ksp1::kanMX4 ptc1::nat1***	TA	MAR216 (BY4742 *ptc1::nat1*)	*ksp1::kanMX4*	BY4741
LTR042	***ckb1::kanMX4 ptc1::nat1***	TA	MAR216 (BY4742 *ptc1::nat1*)	*ckb1::kanMX4*	BY4741
LTR045	***ssk2::kanMX4 ptc1::nat1***	TA	MAR216 (BY4742 *ptc1::nat1*)	*ssk2::kanMX4*	BY4741
LTR047	***pkh1::kanMX4 ptc1::nat1***	TA	MAR216 (BY4742 *ptc1::nat1*)	*pkh1::kanMX4*	BY4741
LTR061	***pkh2::kanMX4 ptc1::nat1***	TA	MAR216 (BY4742 *ptc1::nat1*)	*pkh2::kanMX4*	BY4741
LTR062	***pkh3::kanMX4 ptc1::nat1***	TA	MAR216 (BY4742 *ptc1::nat1*)	*pkh3::kanMX4*	BY4741
CCV66	***ypk3::kanMX4 ptc1::nat1***	ptc1 cassette in kinase mutant			
CCV69	***kcc4::kanMX4 ptc1::nat1***	ptc1 cassette in kinase mutant			
CCV77	***prr2::kanMX4 ptc1::nat1***	ptc1 cassette in kinase mutant			

CCV83	***snf1::kanMX4 ptc1::nat1***	ptc1 cassette in kinase mutant
CCV92	***fab1::kanMX4 ptc1::nat1***	ptc1 cassette in kinase mutant
CCV99	***sip2::kanMX4 ptc1::nat1***	ptc1 cassette in kinase mutant
CCV101	***fmp48::kanMX4 ptc1::nat1***	ptc1 cassette in kinase mutant
CCV110	***yck1::kanMX4 ptc1::nat1***	ptc1 cassette in kinase mutant
CCV111	***sch9::kanMX4 ptc1::nat1***	ptc1 cassette in kinase mutant
CCV114	***prk1::kanMX4 ptc1::nat1***	ptc1 cassette in kinase mutant
CCV121	***hal5::kanMX4 ptc1::nat1***	ptc1 cassette in kinase mutant
CCV124	***tor1::kanMX4 ptc1::nat1***	ptc1 cassette in kinase mutant
CCV125	***elm1::kanMX4 ptc1::nat1***	ptc1 cassette in kinase mutant
CCV126	***hsl1::kanMX4 ptc1::nat1***	ptc1 cassette in kinase mutant
CCV129	***ctk1::kanMX4 ptc1::nat1***	ptc1 cassette in kinase mutant
CCV134	***ptk1::kanMX4 ptc1::nat1***	ptc1 cassette in kinase mutant
CCV137	***hog1::kanMX4 ptc1::nat1***	ptc1 cassette in kinase mutant
CCV144	***sky1::kanMX4 ptc1::nat1***	ptc1 cassette in kinase mutant
CCV149	***cla4::kanMX4 ptc1::nat1***	ptc1 cassette in kinase mutant
CCV150	***mck1::kanMX4 ptc1::nat1***	ptc1 cassette in kinase mutant
CCV162	***mek1::kanMX4 ptc1::nat1***	ptc1 cassette in kinase mutant
CCV167	***frk1::kanMX4 ptc1::nat1***	ptc1 cassette in kinase mutant
CCV168	***ypl150w::kanMX4 ptc1::nat1***	ptc1 cassette in kinase mutant
CCV169	***ssn3::kanMX4 ptc1::nat1***	ptc1 cassette in kinase mutant
CCV170	***env7::kanMX4 ptc1::nat1***	ptc1 cassette in kinase mutant
CCV172	***isr1::kanMX4 ptc1::nat1***	ptc1 cassette in kinase mutant
CCV173	***dbf20::kanMX4 ptc1::nat1***	ptc1 cassette in kinase mutant
LTR060	***ire1::kanMX4 ptc1::nat1***	ptc1 cassette in kinase mutant
RP1	***chk1::kanMX4 ptc1::nat1***	ptc1 cassette in kinase mutant
RP3	***rim15::kanMX4 ptc1::nat1***	ptc1 cassette in kinase mutant
RP4	***scy1::kanMX4 ptc1::nat1***	ptc1 cassette in kinase mutant
RP5	***mcp2::kanMX4 ptc1::nat1***	ptc1 cassette in kinase mutant
MAR154	***slt2::kanMX4 ptc1::nat1***	ptc1 cassette in kinase mutant
MAR213	***bck1::kanMX4 ptc1::nat1***	ptc1 cassette in kinase mutant
CCV68	***vps15::kanMX4 ptc1::nat1***	kinase cassette in *PTC1* mutant
CCV138	***vps34::kanMX4 ptc1::nat1***	kinase cassette in *PTC1* mutant
LTR009	***mkk2::kanMX4 ptc1::nat1***	kinase cassette in *PTC1* mutant

LTR010	***iks1::kanMX4 ptc1::nat1***	kinase cassette in *PTC1* mutant
LTR011	***ste20::kanMX4 ptc1::nat1***	kinase cassette in *PTC1* mutant
LTR014	***tpk3::kanMX4 ptc1::nat1***	kinase cassette in *PTC1* mutant
LTR018	***pkp2::kanMX4 ptc1::nat1***	kinase cassette in *PTC1* mutant
LTR019	***nnk1::kanMX4 ptc1::nat1***	kinase cassette in *PTC1* mutant
LTR020	***ssk22::kanMX4 ptc1::nat1***	kinase cassette in *PTC1* mutant
LTR021	***tpk1::kanMX4 ptc1::nat1***	kinase cassette in *PTC1* mutant
LTR028	***mkk1::kanMX4 ptc1::nat1***	kinase cassette in *PTC1* mutant
LTR030	***sks1::kanMX4 ptc1::nat1***	kinase cassette in *PTC1* mutant
LTR031	***ygk3::kanMX4 ptc1::nat1***	kinase cassette in *PTC1* mutant
LTR036	***cmk1::kanMX4 ptc1::nat1***	kinase cassette in *PTC1* mutant
LTR037	***ste11::kanMX4 ptc1::nat1***	kinase cassette in *PTC1* mutant
LTR038	***smk1::kanMX4 ptc1::nat1***	kinase cassette in *PTC1* mutant
LTR039	***fpk1::kanMX4 ptc1::nat1***	kinase cassette in *PTC1* mutant
LTR043	***rim11::kanMX4 ptc1::nat1***	kinase cassette in *PTC1* mutant
LTR044	***npr1::kanMX4 ptc1::nat1***	kinase cassette in *PTC1* mutant
LTR046	***fus3::kanMX4 ptc1::nat1***	kinase cassette in *PTC1* mutant
LTR048	***cka1::kanMX4 ptc1::nat1***	kinase cassette in *PTC1* mutant
RP2	***ste7::kanMX4 ptc1::nat1***	kinase cassette in *PTC1* mutant

Table S2. Oligonucleotides used in this work

Oligo	Sequence	Use
FPTC1	CCCGGGGGGATCCATGAGTAATCATTCTGAAATC	Gst-Ptc1 overexpression
RPTC1	CCCGGGTTAGGATCCGAGGAAGACAACCATGACCG	Gst-Ptc1 overexpression
FNBP2	CCCGGGGGGATCCATGGCAACGATGGAAACGACC	Gst-Nbp2 overexpression
RNBP2	CCCGGGTTAGGATCCATCCGATATATCTAATTTTGTTTTC	Gst-Nbp2 overexpression
FBCK1	CCCGGGGAAGCTTCCTGCTCCTCTCACCTCAG	pYES3-*BCK1*^{CT} plasmid construction
RBCK1	CCCGGGTTAAAGCTTTTCAGTTTTATTCTCCTGAGAGG	pYES3-*BCK1*^{CT} plasmid construction
FMKK1	CCCGTCGACTCGAGATGGCTTCACTGTTCAGACC	pEG(KG)-MKK1^{S386P} plasmid construction
RMKK1	CCCGTCGACTTAATCTTTCCAGCACTTCC	pEG(KG)-MKK1^{S386P} plasmid construction
Ptc1_pGEX-Fw	CGGGATCCATGAGTAATCATTCTGAAATC	pGEX-6P1-PTC1 construction for expression of GST-Ptc1 in *E. coli*
Ptc1_pGEX-Rv	CGCGTCGACTTAGAGGAAGACAACCATGAC	pGEX-6P1-PTC1 construction for expression of GST-Ptc1 in *E. coli*